Quantified vertical motions and tectonic evolution of the SE Pyrenean foreland basin

J. VERGÉS[1,2], M. MARZO[1], T. SANTAEULÀRIA[1], J. SERRA-KIEL[1],D. W. BURBANK[3], J.A. MUÑOZ[1] & J. GIMÉNEZ-MONTSANT[4]

[1]*Grup de Geodinàmica i Anàlisi de Conques, Departament de Geologia Dinàmica, Geofísica i Paleontologia, University of Barcelona, Martí i Franquès s/n, 08071 Barcelona, Spain*

[2]*Present address: Institute of Earth Sciences 'Jaume Almera' Solé i Sabarís, s/n 08071 Barcelona, Spain (e-mail: jverges@ija.csic.es)*

[3]*Department of Earth Sciences, University of Southern California, Los Angeles, CA 90089-0740, USA*

[4]*Department of Geology, Royal Holloway, University of London, Egham, Surrey TW20 0EX, UK*

Abstract: Local isostatic backstripping analysis is performed across the eastern part of the Ebro foreland basin between the Pyrenees and the Catalan Coastal Ranges. The subsidence analysis is based on two well-dated field-based sections and four oil-wells aligned parallel to the tectonic transport direction of the eastern Pyrenean orogen. The marine infill of the foreland basin is separated into four, third-order, transgressive–regressive depositional cycles. The first and second depositional cycles are located in the Ripoll piggy-back basin and the third and fourth ones are located south of the syn-depositional emergent Vallfogona thrust. Subsidence curves display a typical convex-up shape with inflection points recording the onset of rapid tectonic subsidence. Inflection points coincide roughly with the base of depositional cycles. Rates of tectonic subsidence are less than 0.1 mm a^{-1} in distal parts of the basin and up to 0.53 mm a^{-1} in proximal parts during second depositional cycle. Younger depositional cycles show maximum rates of tectonic subsidence of 0.26 mm a^{-1}. The locus of subsidence within the basin migrated southward at a rate of *c.* 10 mm a^{-1}. This flexural wave crossed the complete Ebro foreland basin in 10–11 Ma. The intraplate Catalan Coastal Ranges at the southeastern margin of the Ebro foreland basin produced an increase of tectonic subsidence rate at 41.5 Ma. Maximum rates of tectonic subsidence coincide with deep-marine infill of the basin, maximum rates of shortening and thrust front advance, and low topographic relief orogenic wedge. Transgressive–regressive depositional cycles can be controlled partly by reductions of available space within the basin during tectonic thickening of the sedimentary pile by layer parallel shortening, folding and thrusting.

Although much less constrained, an approximation of post-thrusting exhumation and isostatic and tectonic uplift, as well as a first determination of possible amounts of eroded material of parts of the Ebro basin illustrate the impact of post-depositional erosion and uplift on the foreland.

The geometry and distribution of the infill of a flexural foreland basin register the interplay between different surficial and deep geological processes and are dependent on the ratio between rates of sediment supply and space available in the basin. Rates of tectonic growth and denudation control sediment supply, mainly in the orogenic wedge, whereas lithospheric strength, advancing tectonics and sea-level variations control the accommodation space in the foreland basin. All these factors are linked to define a unique linkage between orogenic evolution and the foreland basin during several tens of millions of years. However, most foreland basins evolve in a similar way, from marine and largely underfilled to continental, overfilled and largely bypassing (e.g. Allen *et al.* 1986; Fig. 1). The Alpine Molasse basin (Homewood *et al.* 1986; Sinclair & Allen 1992) and the Pyrenees (Puigdefàbregas *et al.* 1986, 1992) as part of the western European foreland basins show good examples of this general evolutionary trend. The internal distribution of sediments within the basin is characterized by several depositional cycles with a duration of a few millions of years (third-order depositional cycles).

VERGÉS, J., MARZO, M., SANTAEULÀRIA, T., SERRA-KIEL, J., BURBANK, D. W., MUÑOZ, J. A. & GIMÉNEZ-MONTSANT, J. 1998. Quantified vertical motions and tectonic evolution of the SE Pyrenean foreland basin. *In:* MASCLE, A., PUIGDEFÀBREGAS, C., LUTERBACHER, H. P. & FERNÀNDEZ, M. (eds) *Cenozoic Foreland Basins of Western Europe.* Geological Society Special Publications, **134**, 107–134.

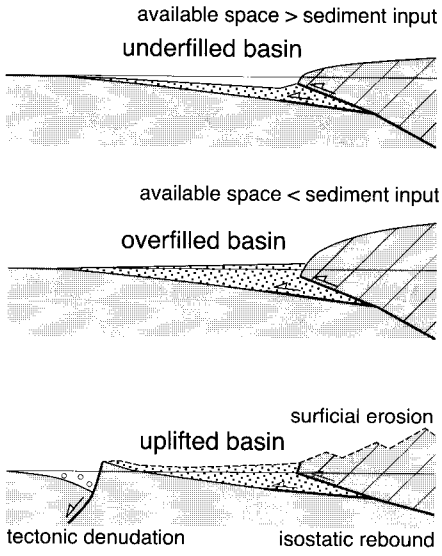

Fig. 1. Vertical motions in a foreland basin during thrusting are governed by the downward flexure of the plate produced by tectonic loads. The large-scale infill distribution on the foreland basin is dependent on the ratio between available accommodation space within the basin and the volume of sediment influx. For low sediment input the basin will be underfilled (Flysch stage). For large sediment influx, the basin will be overfilled (Molasse stage). Post-orogenic vertical motions are mainly controlled by the interplay between tectonic and surficial denudation with concomitant isostatic rebound.

In this paper we present the depositional organization of the Palaeogene marine infill of the southeastern Pyrenean foreland basin together with a quantitative analysis of vertical motions within the basin. This work has been possible by the integration of surface data, oil-well data and non-published commercial seismic lines. An important effort has been made in refining the chronostratigraphic framework of this part of the Pyrenean basin by combining magnetostratigraphic and new palaeontological data. Furthermore, a backstripping analysis, based on local isostatic compensation, has been made across a N–S transect throughout the complete foreland basin. This approach allows us to calculate rates of total and tectonic subsidence in single localities as well as their migration across the basin, ahead of the forelandward-moving Pyrenean deformational front. Moreover, this analysis illustrates how an active distal margin (the Catalan Coastal Ranges) influenced subsidence distribution and subsidence rates across the basin.

Geological setting

The Pyrenees correspond to the western termination of an orogenic belt formed during the Tertiary closure of the Tethyan Sea located between the converging African and European plates (Fig. 2). The relatively straight and E–W-trending Pyrenean orogen developed by the northern subduction of the Iberian lithosphere beneath Europe as imaged by the deep seismic reflection ECORS-Pyrenees profile (Choukroune *et al.* 1989). The Pyrenees merge eastward with the highly arcuate Alps, which formed above a south-dipping European lithospheric subduction underneath Adria, the northern promontory of the African plate, (ECORS-CROP Deep Seismic Sounding Group 1989). Both orogens are doubly sided with a major foreland basin on top of the lower plate (e.g. Muñoz 1992; Pfiffner 1992). The Ebro basin and the Molasse basin represent the latest evolutionary stage of the flexural foreland basin. Earlier foreland basin strata are preserved in piggyback basins on top of thrust sheets. The Aquitaine basin developed on the northwestern side of the Pyrenees and represents a retro-foreland basin.

The eastern side of the Ebro basin displays an irregular shape bounded by the Pyrenees to the north and the Catalan Coastal Ranges to the southeast (Fig. 3). This irregular geometry is due to both the oblique trend of the Catalan Coastal Ranges with respect to the Pyrenean chain and the succession of frontal and oblique segments of the Pyrenean front, inherited from the Mesozoic extensional basin geometry (Puigdefàbregas *et al.* 1992; Vergés & Burbank 1996). The southeastern Pyrenean foreland basin developed almost entirely over pre-Mesozoic basement and stands in contrast to the more westerly Jaca Basin which developed on top of a detached Mesozoic section (e.g. Séguret 1972; Teixell 1996).

The Vallfogona thrust represents the major thrust boundary between the southeastern Pyrenean thrust sheets and the deformed foreland strata (Fig. 3). The thick Tertiary succession cropping out in the Cadí thrust sheet is folded by the Ripoll syncline (Muñoz *et al.* 1986; Puigdefàbregas *et al.* 1986). The lower segment of this stratigraphic succession represents the northern part of the former south Pyrenean foreland basin whereas the upper segment represents the individualization of this part of the trough as a piggyback basin, the Ripoll basin, after the

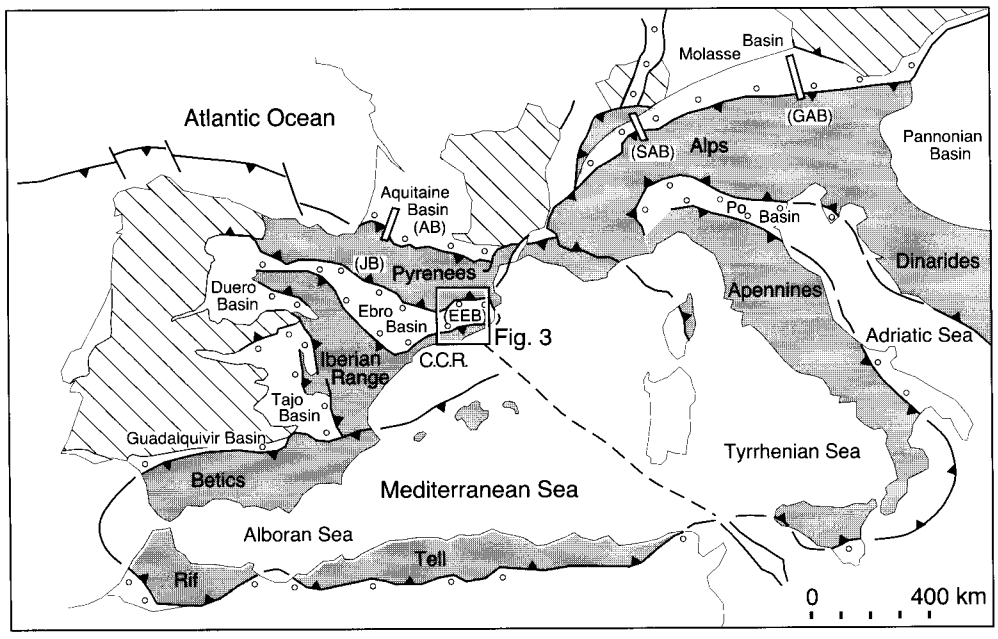

Fig. 2. Tectonic map of western Mediterranean with location of Tertiary orogenic belts and adjacent foreland basins. Thick black lines with black triangles bound shaded orogenic regions. Open circles highlight foreland basins. Oblique lines define major outcrops of basement. Narrow boxes indicate location of compared subsidence studies in the Jaca basin in the western Pyrenees (JB), Aquitaine foreland basin (AB), Swiss Alpine and German Alpine basins (SAB and GAB).

inception of the Vallfogona thrust. A large part of the Ebro foreland basin is deformed by a system of folds and thrusts, in part coeval to deposition (Puigdefàbregas *et al.* 1986; Burbank *et al.* 1992*a*), detached above a suite of foreland evaporitic levels (Vergés *et al.* 1992; Sans *et al.* 1996).

The subsidence analysis presented in this paper has been made along a N–S transect (for location see in Fig. 3), parallel to the tectonic transport direction in this segment of the Pyrenees. The location of the studied stratigraphic sections and oil-wells have been projected into a regional cross-section, presented in Fig. 8 and described in Vergés (1993) and Vergés & Burbank (1996). This projection into the regional section is nevertheless problematic due to the rapid lateral changes in both the stratigraphy and the tectonic style and has to be viewed as an approximate couple between subsidence results and regional fold-and-thrust belt geometry. For instance, the Puig-reig oil-well is projected parallel to the Puig-reig anticlinal structure from the east where the anticline ends and displays a much reduced shortening (Vergés & Burbank 1996).

Depositional cycles and chronostratigraphy

The Palaeogene marine succession of the SE Pyrenean basin has been divided into four major transgressive–regressive depositional cycles across the southeastern Pyrenean foreland basins. First and second cycles are defined within the Ripoll syncline (Cadí thrust sheet in Fig. 4), whereas third and fourth cycles are contained in the Ebro basin (Figs 3 & 4). The lateral continuity of these four cycles throughout the foreland basin is not straightforward. Difficulties arise for the following reasons: (1) the stratigraphic succession is partitioned in different tectonic units and basins as discussed above; (2) the interplay between tectonics and sedimentation occurs at different scales; (3) the Catalan Coastal Ranges represent an active, rather than passive, southern basin margin (Figs 2 & 3); (4) the sediments vary and comprise carbonates, clastics and evaporites; and (5) precise chronostratigraphic control is lacking in the oil-wells of the central part of the basin.

In this situation, an accurate chronostratigraphy is especially needed to determine reliable

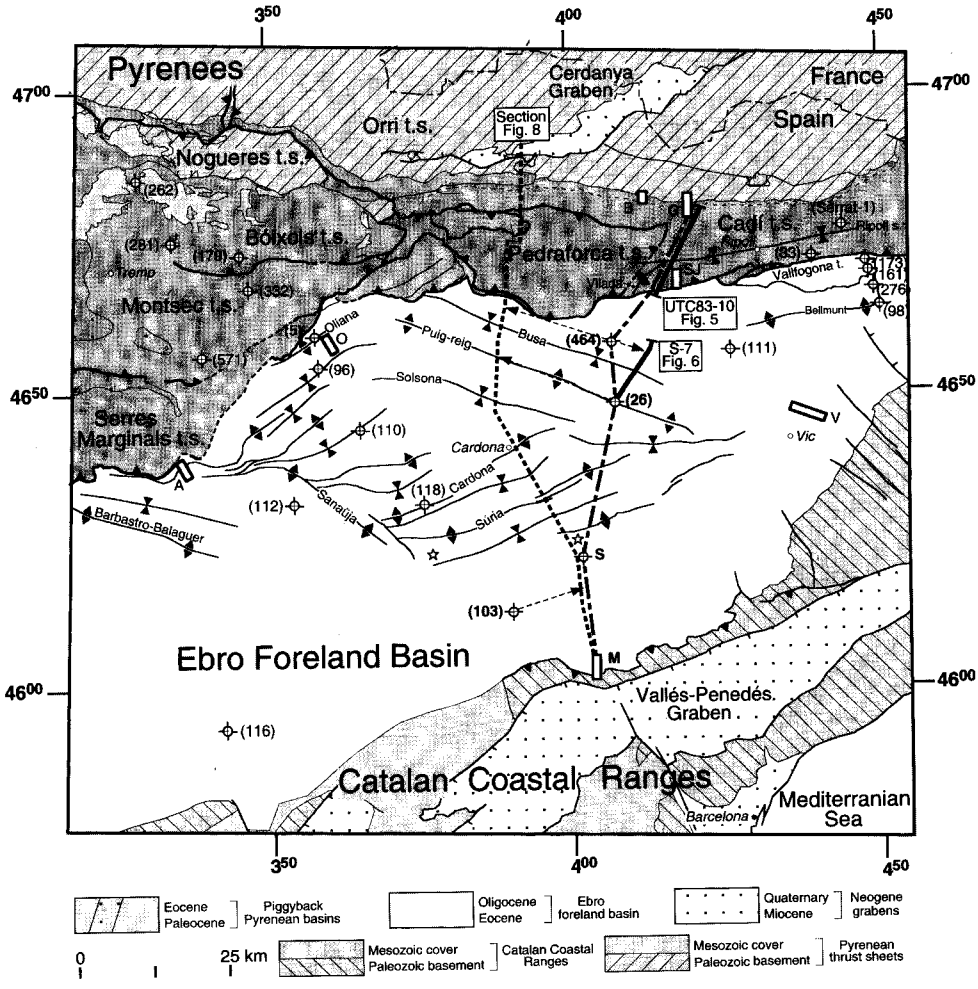

Fig. 3. Structural map of the Eastern part of the Ebro basin between the Pyrenean thrust belt to the North and the Catalan Coastal Ranges to the South. Dashed line shows the analysed transect from G to M. Short thick lines represent the location of seismic lines (UTC83-10 crossing the Cadí thrust sheet and S-7 in the northern side of the Ebro basin). Open circles with crosses show oil-wells with a number referred to an oil-well index published in Lanaja (1987). Thick dashed N–S line shows the position of a regional balanced and restored cross-section (Fig. 8) used in the construction of a crustal-scale section (Vergés *et al.* 1995). Subsidence results have been projected, parallel to the tectonic structures to both the analysed section to the east and to the regional cross-section to the west (see black dashed arrows). Sections and oil-wells used in this study are represented by G-Gombrèn section; (464), Jabalí oil-well; (26), Puig-reig oil-well; S, Santpedor oil-well; (103), Castellfollit oil-well; and M, Montserrat section. Additional locations are represented by V, Vic section; SJ, Sant Jaume de Frontanyà section; B, Bagà section; O, Oliana section; and A, Artesa del Segre section. Little stars show location of vitrinite samples used in this study (Santpedor and Calaf localities).

depositional cycles boundaries (Fig. 4). Chronostratigraphy is based on biostratigraphic and magnetostratigraphic data compilation from published works and their correlation to the magnetic polarity time scale. Biostratigraphy is based mainly on larger foraminifera, especially *Nummulites* and *Alveolina* (Hottinger 1960; Ferrer 1971; Schaub 1981; Serra-Kiel 1984; Tosquella 1995). Magnetostratigraphic data come from seven different sections within the studied region (Fig. 3; Burbank *et al.* 1992*a*,*b*; López-Blanco *et al.* in press) as well as from the central Pyrenees where the Palaeocene–Eocene boundary is well defined in the Campo section

(Serra-Kiel *et al.* 1994). The correlation between magnetic sections and larger foraminifera corresponding to Shallow Benthic Zones (SB), mainly based on south Pyrenean specimens (Serra-Kiel *et al.* in press) is shown in Fig. 4. The magnetic polarity time scale of Cande & Kent (1995) is used here.

Ages corresponding to either transgressive–regressive boundaries or lithological formations are calculated by interpolation assuming constant rates of sediment accumulation during well-defined magnetic intervals. The use of lithostratigraphic formations minimize the possible changes of sediment accumulation rates within analyzed intervals. Ages of the successions derived from oil-wells have been calculated from biostratigraphic data, correlation with surface sections, and the support of the magnetostratigraphic sections of Vic (Burbank *et al.* 1992*a*) and Oliana (Burbank *et al.* 1992*b*), corresponding to the basin centre (Fig. 3). The age for the uppermost part of the Bellmunt deposits in the Gombrèn section has been calculated by extrapolating the mean sediment accumulation rate determined for the interval 45.82–43.78 Ma. The age of the uppermost deposits of the Solsona Fm in the Jabalí, Puigreig, Santpedor and Castellfollit sections have been determined assuming mean sedimentation rates of 0.23 mm a^{-1} determined from roughly coeval deposits in Oliana (Burbank *et al.* 1992*b*) and in Artesa del Segre (Meigs *et al.* 1996) (see Fig. 3).

During the Palaeogene, the inception of marine conditions on the SE Pyrenean foreland basin occurred above a regional unconformity dated as 55.9 Ma old in the Campo section (chron 24.3r; Serra-Kiel *et al.* 1994) as well as farther west in the Urbasa section, Basque country (Pujalte *et al.* 1994). First depositional cycle is Ilerdian to early Cuisian in age comprising SB5 to SB10 based on magnetostratigraphy (Serra-Kiel *et al.* 1994; Bentham & Burbank 1996) correlated with biostratigraphic data (Serra-Kiel *et al.* 1994). This first transgressive–regressive depositional cycle started with shallow-marine Alveolina limestones (Cadí Fm), Ilerdian and Cuisian in age. The age of the base of the Cadí Fm decreases toward the distal margin of the basin: early Ilerdian in the Pyrenean thrust sheets, middle Ilerdian in the centre of the Ebro basin and middle Ilerdian 2 in the southern and distal margin (Orpí Fm). The shallow-marine carbonate platform represented by both the Cadí and Orpí Formations merged northward into deeper water calcareous mudstones of the Sagnari Fm (Luterbacher *et al.* 1991; Giménez-Montsant 1993). The regressive hemicycle is represented by a prograding, deltaic, clastic wedge capped by fluvio-lacustrine facies of the Corones Fm. (Giménez-Montsant 1993), early Cuisian in age (Tosquella 1995). Based on the magnetostratigraphic studies, the total duration of this transgressive–regressive cycle is 5.1 Ma (from 55.9 to 50.8 MaBP).

In the Pyrenean thrust sheets, the second cycle is mid-Cuisian to early Lutetian in age containing SB11 to SB13 based on magnetostratigraphy (Bentham & Burbank 1996) correlated with biostratigraphy (Samsó *et al.* 1994; Tosquella 1995). This cycle starts with shallow-marine limestones (uppermost part of the Corones Fm), which rapidly grade upward into a *c.* 1000 m thick, slope facies association mostly represented by carbonates and calcareous mudstones, often slumped (Armàncies Fm). This slope association includes up to seven, decametric, megabreccia units interpreted as the result of slope resedimentation of co-existing carbonate platforms which constitute the Penya Fm (Giménez-Montsant 1993). Above the slope marls, over 700 m of siliciclastic turbidites (Campdevànol Fm), linked to southward-prograding fluvio-deltaic and fan-delta systems (lowermost part of the Bellmunt Fm), are present in the northern margin of the Cadí thrust sheet. These turbidites filled a trough adjacent to the advancing Pyrenean thrust sheets and was rimmed southward by the above mentioned carbonate platform (Puigdefàbregas *et al.* 1986). The uppermost part of the turbiditic succession could be interstratified with evaporitic deposits (Martínez *et al.* 1989), although the thick evaporitic alternation was deposited southward of the turbiditic depocentre (Fig. 4). The thickness of this evaporitic unit (Beuda Fm) greatly increases southwards, as evidenced by the Serrat-1 oil-well (Union Texas Inc. 1987), drilled in the northern flank of the Ripoll syncline (Cadí thrust sheet; Fig. 3). In the footwall of the Vallfogona thrust, the well cuts *c.* 2000 m of gypsum, and alternating gypsum, sandstones and marls, with a 200 m thick intercalation of salt (Martínez *et al.* 1989). The 100 m thick level of gypsum cropping out along the northern flank of the Ripoll syncline represents the northern margin of the Beuda depocentre. This second depositional cycle comprises the mid-Cuisian and the latest part of the early Lutetian, spanning a total of 4.54 Ma (from 50.8 to 46.26 MaBP).

The third and fourth marine depositional cycles are exposed south of the Vallfogona thrust, in the Jabalí and Puig-reig oil-wells and in the southern margin of the Ebro basin.

The third cycle is early Lutetian to uppermost Lutetian in age. It contains SB14, SB15 and

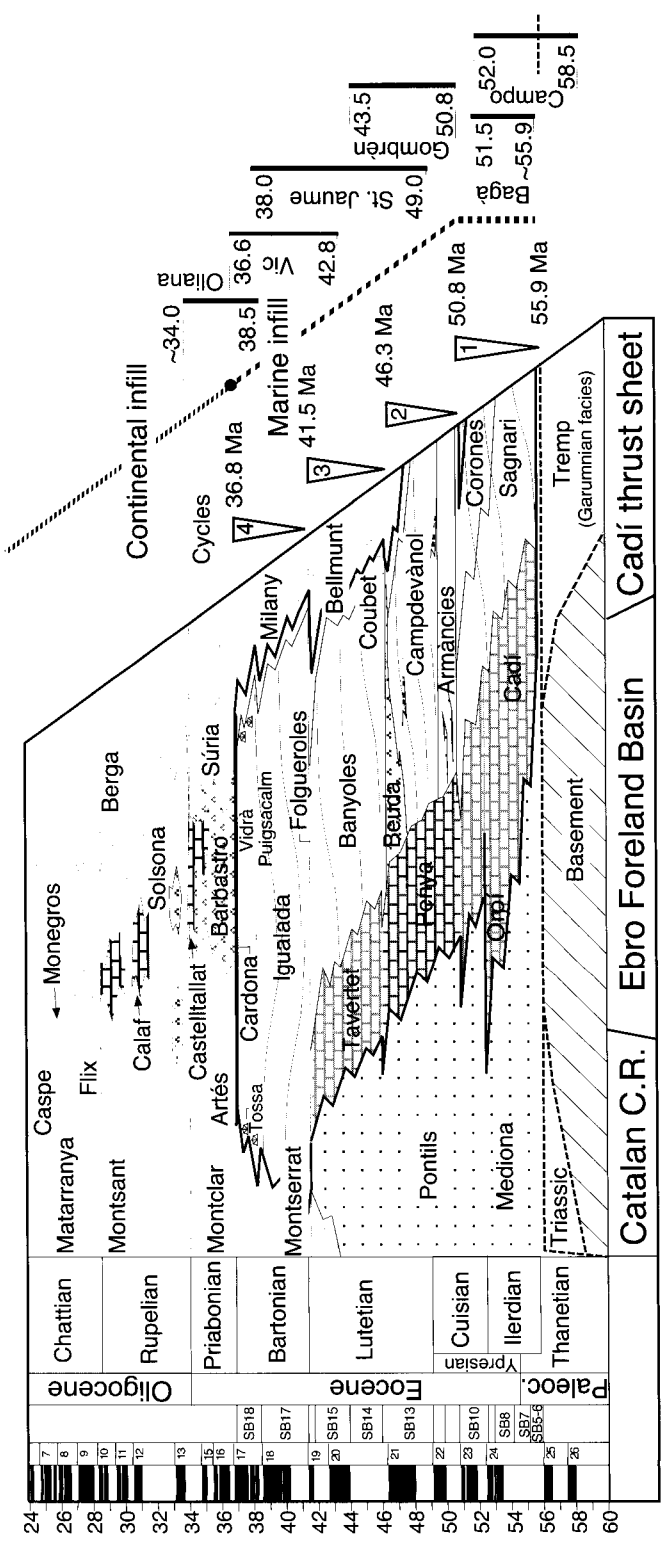

Fig. 4. Stratigraphic panel across the Ripoll basin (Cadí thrust sheet), Ebro foreland basin and Catalan margin. The marine infill of the basin (limited from the continental deposits by a thick continuous line) is separated into four transgressive-regressive third-order depositional cycles of about 5 Ma duration. Biostratigraphic data combined with magnetostratigraphic information define the chronostratigraphic framework of the study area. Magnetostratigraphy comes from Bagà, Gombrèn, Sant Jaume de Frontanyà, Vic and Oliana sections (Burbank *et al.* 1992*a,b*; Vergés & Burbank 1996) and from the Campo section (Serra-Kiel *et al.* 1994). Global polarity time scale from Cande & Kent (1995). Larger foraminifera shallow bentic zones (SBZ) from Serra-Kiel *et al.* (in press).

SB16 zones based on magnetostratigraphy (Burbank *et al.* 1992*a*; Bentham & Burbank 1996) correlated to biostratigraphic data (Serra-Kiel & Travé 1995; Samsó *et al.* 1994). This third cycle starts with a renewed transgression recorded at the northern basin margin by a glauconite-rich, mostly sandy, nearshore-to-deltaic facies association (Coubet Fm) that unconformably overlies previous continental deposits (lowermost part of the Bellmunt Fm). These sandy facies are overlain by a thick, southward-prograding, terrigenous fluvio-deltaic wedge (Mató *et al.* 1994), comprising conglomerates, sandstones and marls (Bellmunt and Banyoles Formations). The thickness of this fluvio-deltaic wedge is around 700 m east of the studied transect (Saula *et al.* 1994), *c.* 600 m in the Jabalí oil-well and only *c.* 200 m in the Puig-reig oil-well. To the south, these fluvio-deltaic clastics overlap a southern carbonate platform (Tavertet Fm). The age of this cycle is well-constrained by both biostratigraphy and magnetostratigraphy; it covers a time span of 4.76 Ma (from early Lutetian at 46.26 to late Lutetian at 41.50 MaBP).

The fourth cycle is Bartonian in age. It comprises SB17 and SB18 zones based on magnetostratigraphy (Burbank *et al.* 1992*a*) integrated with biostratigraphic data (Serra-Kiel & Travé 1995). This fourth depositional cycle is characterized by the absence of well-developed platform carbonate deposits, because of the simultaneous progradation from both basin margins of Montserrat Fm fan-delta deposits in the south and Milany Fm fluvio-deltaic sandstones and conglomerates in the north grading basinward to prodeltaic-offshore marls of the Igualada Fm. The overall offlapping trends of these terrigenous wedges are locally punctuated by minor onlapping transgressive pulses leading to the local and temporary development of carbonate platforms and reef build-ups which become more frequent toward the top of the cycle (Tossa Fm). These mixed terrigenous–carbonate wedges overlie a transgressive, glauconite-rich, shelf sandstone complex (Folgueroles Fm) and are capped in turn by an evaporitic plug (Cardona Fm) that fills up the marine basin. The thickness of this fourth cycle is about 1560 m in the Jabalí oil-well and 1760 m in the Puig-reig oil-well, although a thrust fault located at *c.* 1600 m depth produced tectonic duplication of part of the section that could be up to 450 m determined from vitrinite reflectance data from the Puig-reig oil-well (Clavell 1992). If these determinations are correct, there would be an overestimation of both total sedimentary thickness and calculated value and rate of subsidence for this interval. However, this tectonic duplication is not represented in the seismic line S-7 projected from the eastern termination of the Puig-reig anticline (see Fig. 6).

South of the Vallfogona thrust, the fourth sedimentary cycle shows two internal angular unconformities located at the base and within the cycle. These two unconformities fossilize older folds and thrusts and are subsequently folded and thrusted (Mató *et al.* 1994). These cross-cutting relationships suggest continuous deformation in the south Pyrenean frontal thrust zone (at the time slices we are considering) at least during the total duration of the last marine cycle, which is estimated to be 4.7 Ma (Bartonian, from 41.5 to 36.8 MaBP).

The above described depositional cycles are not recognizable, except the fourth one, at the southern margin of the Ebro foreland basin near the contact with the Catalan Coastal Ranges (Fig. 4). In this sector the carbonate platform deposits (Cadí-Orpí, Penya, and Tavertet Formations) are substituted by continental red beds (Pontils Group, Mediona and Cairat Fms). The precise chronostratigraphic attribution of these continental units is not well-constrained, and the possible existence of several major stratigraphic gaps, although suspected, can not be proved.

Two seismic lines have been selected to show the geometry of the Ripoll piggyback basin, the position of the underlying Vallfogona thrust (seismic line UTC-83-10; Fig. 5), and the geometry of the southward prograding shallow-water carbonate platforms in the central northern part of the Ebro foreland basin (seismic line S-7; Fig. 6).

Cadí thrust sheet structure: seismic line UTC-83-10

Line UTC-83-10 (Union Texas España Inc. 1983, migrated) shows the geometry of the Cadí thrust sheet and underlying tectonic units (Fig. 5). The line is NNE–SSW oriented, crosses the Cadí thrust sheet but remains parallel to the southern flank of the Vilada anticline in the southern part of the line. This anticline plunges toward the NNE as a result of a folding interference with the Ripoll syncline (Vergés *et al.* 1994). The Vilada anticline is parallel to the eastern oblique termination of the lower Pedraforca thrust sheet and synchronous to its emplacement and further development (Martínez *et al.* 1988; Burbank *et al.* 1992*a*). The southern end of the seismic line is parallel to and located 1 km northward of the present outcrop of the Vallfogona thrust (Fig. 3).

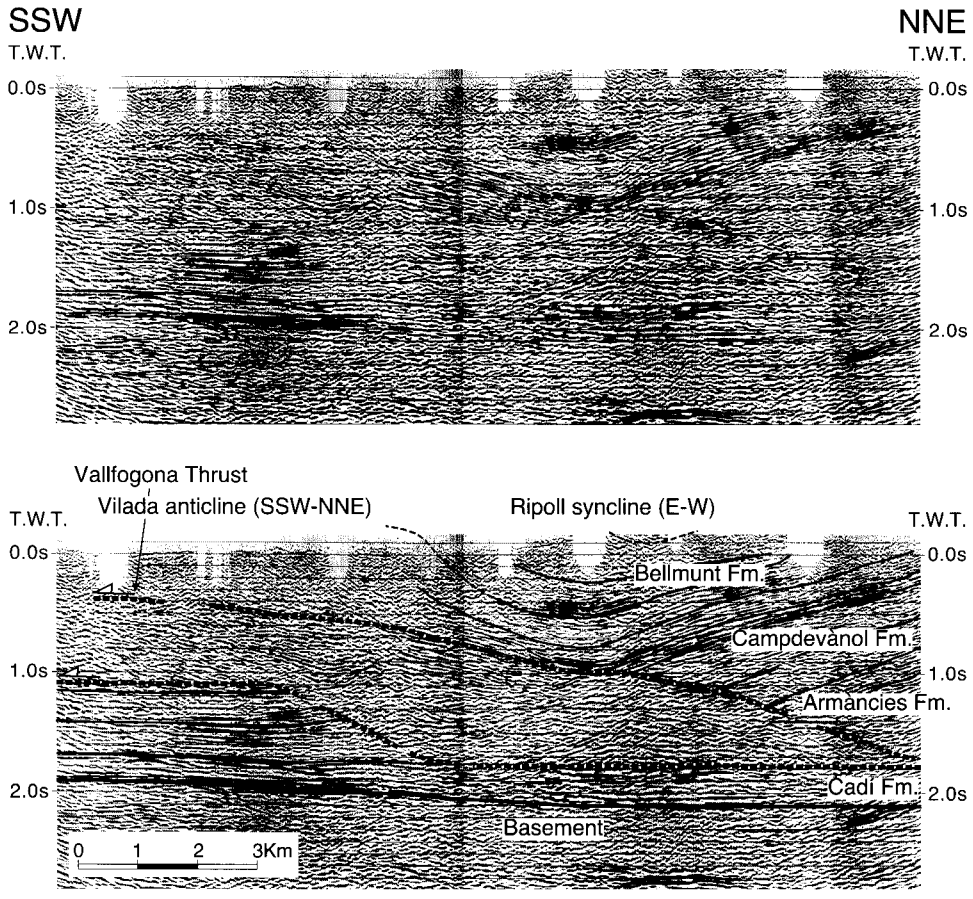

Fig. 5. Seismic line UTC-83-10 (Union Texas España Inc., 1983, migrated) and interpreted line drawing. The line parallels the eastern oblique termination of the Pedraforca thrust sheet and the Vilada anticline in its southern part as shown in Fig. 3. The line shows the geometry of asymmetric Ripoll syncline on top of the Vallfogona thrust that define the Cadí thrust sheet. The thrust showing a ramp geometry between two flat segments in the footwall of the Vallfogona thrust represents the main detachment level within the deformed Ebro basin. Vertical and horizontal scales are similar.

An almost parallel and gently north-dipping group of reflectors, interpreted as the lower Eocene carbonate platforms (Cadí Fm), characterizes the bottom part of the line between 1.75 and 1.9 s (TWT) to the south. Above these reflectors, the line shows three different panels of reflectors that, from north to south, define (a) the Ripoll syncline (as part of the Cadí thrust sheet) above the Vallfogona thrust, (b) an intermediate unit in the footwall of the Vallfogona thrust, and (c) nearly flat-dipping and parallel reflectors in the southern part of the line between 1.1 and 1.75 s.

The Ripoll syncline displays a highly asymmetric geometry characterized by a complete and thick south-dipping Palaeocene–Eocene stratigraphic section in the northern flank whereas only the uppermost part of these deposits crop out in the southern flank. The cut-off relationships between the Ripoll syncline strata and the underlying Vallfogona thrust can be expressed as follows: the northern flank of the syncline represents a high angle hanging wall ramp with respect the Vallfogona thrust whereas the hinge zone and the southern flank of the syncline represent a very low angle hanging wall ramp. The Ripoll syncline shows a northward migration of its axis through time. The footwall of the Vallfogona thrust is characterized by short and irregular reflectors interpreted as a set of folds and thrusts that crop out to the south of the Vallfogona thrust (Muñoz *et al.* 1994; Mató *et al.*

1994). Well-imaged subhorizontal reflectors located in the southernmost part of the seismic line between 1.1 and 1.75 s display an abrupt northern termination interpreted as the footwall ramp of a north-dipping and south-directed thrust related to the foreland fold and thrust system. This thrust can be followed in the regional cross-section, although, the geometry of the Cadí thrust sheet west of the seismic line shows an important southern tilt due to the emplacement of basement tectonic units in the northern part of the section (Vergés *et al.* 1995; see Fig. 8).

Ebro foreland basin structure: seismic line S-7

Line S-7 (UERT, S.A. 1977, fold stack) shows the geometry and distribution of shallow-marine prograding platforms in the central-northern segment of the Ebro foreland basin (Fig. 6). The line with a NNE-SSW direction, crosses the gentle Busa syncline and ends at the Puig-reig oil-well in the northern flank of the Puig-reig anticline. The Jabalí oil-well has been projected into the S-7 line from 6 km to the WNW, parallel to the northern flank of the Busa syncline (Fig. 3).

The seismic line shows different vertical segments according to their seismic facies reflectivity (Fig. 6). The lower segment is composed of subhorizontal, parallel and non-deformed group of reflectors between 1.3 and 1.0 s to the south of the line. The southern ends of these reflectors display a progressive southward onlap over a less reflective level interpreted as the basement (upward arrows in Fig. 6). The northern ends of individual reflectors grade laterally and northward into the overlying less reflective segment, corresponding to more fine grained sediments (downward arrows in Fig. 6). The lowermost reflectors correspond to the lower and middle Eocene platform limestones (Fig. 4) as confirmed by well information (Jabalí and Puig-reig oil-wells). The length of individual reflectors is on the order of few tens of kilometres. The less reflective segment, located between 1.05 and 0.85 s (at the southern part of the line) shows increasing reflectivity toward the north and has been interpreted as corresponding to marls and sandstones of the Banyoles Fm. Between 0.85 and 0.5 s, there is a reflective segment delineating the Busa syncline and corresponding to the upper part of the Igualada Fm. The uppermost segment, above 0.5 s is much less reflective although individual reflectors outline the syncline geometry. These reflectors correspond to the fluvial pelites, sandstones and conglomerates of the Solsona Fm.

Sedimentary model and palaeobathymetries

Figure 7 shows the interpretation of the studied part of the foreland basin. The shallow-water platform limestones migrate and become thinner toward the south. The northern Jabalí oil-well cuts through *c.* 820 m of limestones (Cadí to Tavertet Formations) and about 600 m of overlying terrigenous deposits (Banyoles Fm), whereas the southern Puig-reig oil-well cuts across *c.* 480 m of limestones and *c.* 200 m of marly deposits. The fluvio-deltaic Banyoles Fm passes southward and overlaps the platform deposits. Although the ages of these platforms are not well constrained across the whole basin, seismic information shows that the uppermost well-imaged reflector cut in the Jabalí oil-well corresponds to the middle part of the group of reflectors cut in the Puig-reig oil-well, indicating therefore a fairly rapid southward migration of the shallow marine platform systems, as well as a younger age for the base and top of these carbonate platforms in the same direction (Fig. 7).

The south-dipping geometry of some of the reflectors corresponding to the Banyoles Fm can be interpreted as depositional slopes. Nevertheless, the regional tectonic framework indicates that there is a regional detachment level that follows approximately the contact between limestones and marls (Vergés *et al.* 1992; Sans *et al.* 1996). This detachment climbs up from the limestone–marl contact to the Cardona salt horizon and produces the Puig-reig anticline above the thrust ramp.

Facies distribution within the basin shows an inner, northern part characterized by thick marine terrigenous wedges grading southward to shallow-water carbonate platforms, overlapping thin continental deposits located on the unflexed part of the foreland basin (Fig. 4). Foreland basin carbonate platforms on the southern margin migrated toward the foreland side of the basin although several progradational episodes toward the inner part of the basin are recorded by at least seven megabreccia units during the second depositional cycle. These megabreccias are intercalated with talus marls cropping out in the northern flank of the Ripoll syncline (Puigdefàbregas *et al.* 1986; Barnolas 1992; Giménez-Montsant 1993). Above the talus deposits, important north-derived turbiditic wedges (Campdevànol Fm) produced the shift of depositional facies belts to the south. The end

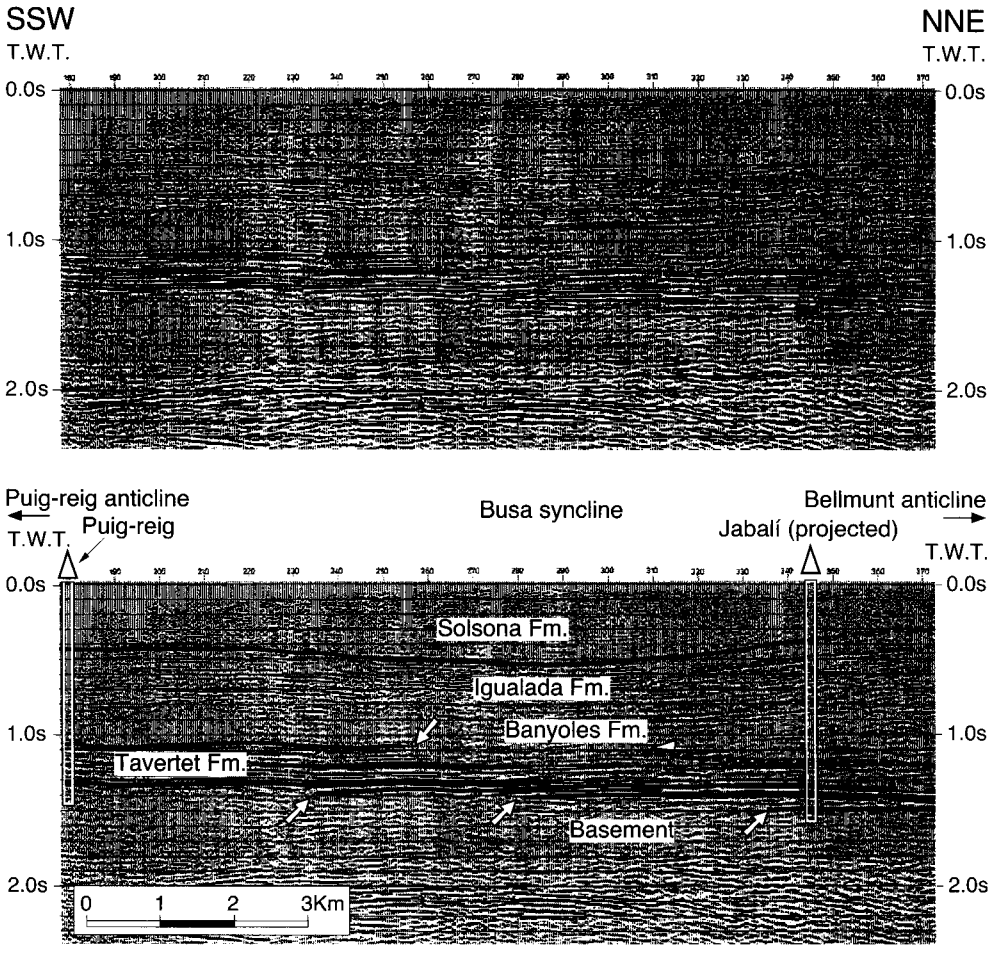

Fig. 6. Seismic line Seismic line S-7 (UERT, S.A., 1977, fold stack) and interpreted line drawing. The line is NNE-SSW and crosses the Busa syncline to the north and the Puig-reig anticline to the south as shown in Fig. 3. The line shows the geometry of the northern part of the Ebro basin, especially the southward migration of the lower and middle Eocene shallow marine platform limestones (constrained by Jabalí and Puig-reig boreholes), represented by the lower set of subhorizontal reflectors of the line. Arrows point to the northern and southern ends of individual reflectors. Upward-pointing-arrows indicate the southward migration of platforms. Vertical and horizontal scales are similar.

of carbonate platform development during the fourth cycle coincides with the onset of generalized clastic deposition by large fan-delta and fluvio-deltaic complexes around the Ebro basin (Fig. 4).

These relationships between carbonate platforms and clastic wedges are well exposed along the N–S, forelandward direction of facies migration in the Jaca piggyback basin (JB in Fig. 2). Shallow-water carbonate platforms developed in the distal margin of the Jaca basin, whereas a thick unit of northerly derived siliciclastic turbidites (Hecho Group) filled the basin during a 9–10 Ma long interval spanning from Ypresian to late Lutetian (e.g. Labaume *et al.* 1985; Barnolas & Teixell 1994). Eight megabreccia units are recognized within the turbidites, interpreted as single depositional events produced by either episodes of thrusting in the northern side of the trough (Johns *et al.* 1981; Labaume *et al.* 1985) or episodes of drowning and collapse of the southern carbonate platform during the migration of the tectonic flexure toward the foreland side of the basin (Barnolas & Teixell 1994). The southern depocenter migration during this period of time was 3–5 mm a^{-1} (Labaume *et al.* 1985; Barnolas & Teixell 1994).

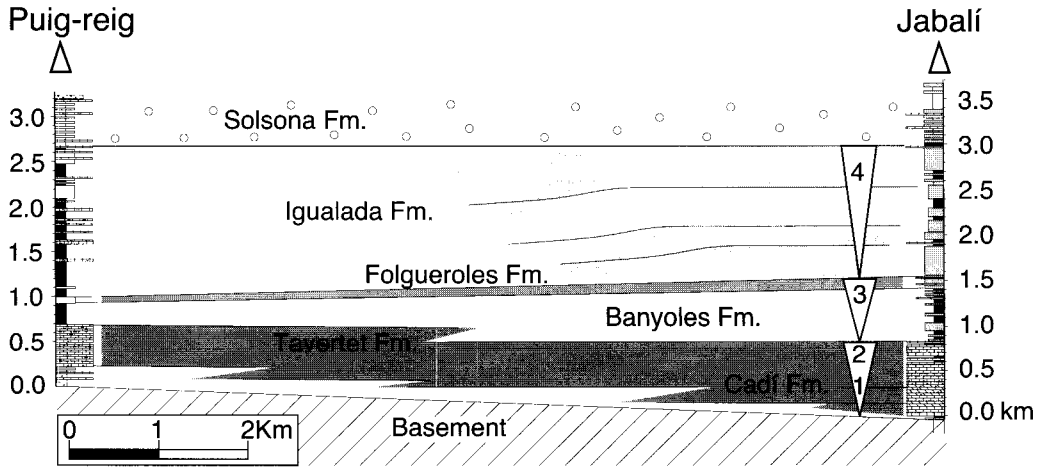

Fig. 7. Interpretative stratigraphic panel from Jabalí to Puig-reig oil-wells supported by seismic data. The lower and middle Eocene limestones migrate toward the foreland coevally with the migration of the foreland flexure. Triangles represent depositional cycles.

Palaeobathymetry is an important factor in subsidence analysis. For this reason we utilize multiple approaches to estimate palaeowater depths. Palaeobathymetries of southeastern Pyrenean foreland platform and shallow-water deposits are well constrained by larger foraminifera fossil record. At present, *Alveolina* develop between 10 and 60 m depth and are especially abundant between 25 and 35 m whereas the range of *Nummulites* is between 30 and 130 m with their maximum abundance at 45–85 m (Hottinger 1977; Reiss & Hottinger 1984). The palaeobathymetric values for the Armàncies and Campdevànol Fms presents more uncertainties because they lack good palaeobathymetric indicators. Planktonic foraminifera, are almost absent in these sediments. Within the Armàncies Fm and in the front of carbonate platforms, the megabreccias extend for around 20 km along the strike of the basin centre (Vergés *et al.* 1994; Muñoz *et al.* 1994), as other modern analogs in active tectonic settings, that extend along 30 km downslope and 16 km along the axis of the basin (Hine *et al.* 1992). This modern-analogue massive deposition occurred above slopes of 2.4°, reaching depths of up to 300 m. Although it is difficult to compare different tectonic scenarios, we think that the second depositional cycle follows a deepening–shallowing pattern, starting at very shallow depth of *c.* 15 m above the upper layer of the Corones Fm and increasing the depth to the base of the Campdevànol turbidites at a maximum depth of *c.* 300 m. From this point, there is a shallowing sense of the bathymetry, very well constrained by a *Turritella* horizon, located on the lowermost part of the Beuda Fm (deposited around 50 m below sea level), to the final very shallow-water or even subaerial exposure at the top of the Beuda evaporites (Ortí *et al.* 1988). Although a more precise palaeobathymetric analysis would be desirable, especially for the Armàncies and Campdevànol Formations, the values discussed above give us adequate lower and upper palaeobathymetric boundaries for the subsidence analysis presented below (Table 1).

Palaeobathymetry is less constrained for continental deposits. We assumed an average altitude of 50 m (0 to –100 m) above sea level for Bellmunt and Solsona fluvial deposits. Fluvial sediments of the Bellmunt Fm were deposited, at least partially, after the Ripoll basin become a piggyback basin on top of the Vallfogona thrust. However, the Ripoll basin was not completely disconnected from the main foreland basin to the south where marine sedimentation represented by the Coubet and Banyoles Fms prevailed during this interval (Muñoz *et al.* 1994; Saula *et al.* 1994). Alluvial and fluvial Solsona deposits in the basin centre were deposited after the closure of the south Pyrenean foreland basins toward the Atlantic Ocean at the Bartonian–Priabonian boundary. These deposits produced an extensive backfilling of the basin and external parts of the Pyrenean thrust belt (Coney *et al.* 1996) that could be concurrent with a continuous increase of the palaeobathymetry within the basin. However, we assumed a fairly low altitude between 0 and 100 m above sea level

Table 1. *List of initial parameters used in this subsidence analysis for each lithology (rock densities, initial porosities and porosity coefficients)*

Lithology	Shales	Siltstones	Sandst.	Cong.	Marls	Limest.	Gypsum	Anhydrite
Initial Porosity ϕ_0	0.63	0.59	0.49	0.5	0.58	0.5	0.5	0.5
Constant c (m^{-1})	0.00051	0.00045	0.00027	0.0003	0.00059	0.0007	0.0009	0.0009
Density (g cm^3)								
General	2.50	2.53	2.60	2.60	2.50	2.67	2.31	2.85
Garumnian		2.51	2.54			2.67		
Cadi Fm						2.69		
Orpi Fm						2.65		
Sagnari Fm					2.58			
Corones Fm			2.62		2.56	2.66		
Amàncies Fm					2.50	2.60		
Campdevànol Fm		2.55	2.69		2.48			
Beuda Fm								2.85
Igualada Fm					2.35			
Solsona Fm			2.53					

for the Solsona Fm deposits (Table 2). Finally, above sea-level palaeobathymetries for Montserrat fan-delta deposits are deduced from the fan-delta palaeotopographic reconstructions (López-Blanco *et al.* in press; Table 2).

Subsidence analysis

Subsidence analysis is made along a N–S profile, parallel to the direction of the Pyrenean tectonic transport, along the southeastern Pyrenean foreland basin from the Ripoll piggyback basin in the north to the Catalan Coastal margin of the Ebro basin in the south (Figs 3, 8). Local isostatic backstripping analysis is carried out on six detailed stratigraphic sections along this N–S transect. The northernmost, outcrop-based, Gombrèn stratigraphic section spans the northern flank of the Ripoll syncline (Cadí thrust sheet). The presented section is based on a detailed unpublished section from UERT, S.A. (1977) shown in Fig. 8. The section records the continental Palaeocene section that underlies the first and second depositional cycles and is combined with good magnetic time-control for the Eocene sequence (Bagà and Gombrèn magnetostratigraphic sections; Burbank *et al.* 1992*a*; Fig. 3). South of the Vallfogona thrust, in the northern crops out of the Ebro basin, the Jabalí and Puig-reig oil-wells cut the complete Eocene marine depositional sequence (first to fourth cycles). The Santpedor and Castellfollit oil-wells characterize the central and southern margins of the Ebro basin. These two sections, as well as the outcrop-based Montserrat stratigraphic column represent mostly the fourth depositional cycle. The Montserrat section and magnetostratigraphy are based on López-Blanco *et al.* (in press).

The stratigraphic intervals used in this subsidence analysis correspond to lithostratigraphic formations that show fairly homogeneous sedimentary facies. We assume a constant rate of sedimentation within well-constrained intervals of time. The lithological percentages for each interval have been resolved from calculations based on detailed 1:500 sections, except for the Santpedor section in which information was less reliable and the section was incomplete in its upper part corresponding to the Solsona Fm.

This subsidence analysis, assuming Airy isostasy, is made from decompaction calculations and uses estimates of palaeobathymetry. Decompaction calculations are based on van Hinte (1978) using a simple exponential relationship for changes in porosity with depth. Initial porosities and constant *c* are based on Sclater & Christie's (1980) values for detritic and carbonatic rocks and on Sonnenfeld's (1984) values for evaporitic rocks. To determine possible errors during decompaction we calculate decompacted thickness of the section using a more accurate algorithm (Allen & Allen 1990; Angevine *et al.* 1990). The formal errors have been omitted as they are insignificant (a minimum of 1.1% in the Montserrat section to a maximum of 4.6% in the Gombrèn section). The errors associated with the specific choices of porosities and compaction exponent *c* are unknown. They are probably considerably greater than the formal errors cited above, but they are unquantified and are ignored here. Table 1 lists initial porosities and constant *c* for each lithology.

The backstripping technique that allows us to calculate tectonic subsidence is based on Steckler & Watts (1978). We applied specific final densities for both particular lithologies and formations based on regional studies by Rivero (1993) as well as evaporitic rock densities based on Sonnenfeld (1984), that are listed in Table 1. We used 3.3 g cm^{-3} for mantle and 1.0 g cm^{-3} for water densities. Equations for continental basins, in which tectonic subsidence is calculated for an air-loaded basin, rather than a water-loaded basin, are applied to the Montserrat section and decrease the calculated tectonic subsidence by a factor of 30% with respect to marine equations. Nevertheless, we also analysed this section using only marine equations to compare the results.

Conservative estimations of palaeobathymetry for marine and continental deposits have been discussed in the preceding section and are listed in Table 2.

Because the uncertainties on the correlation between sea-level curves and South Pyrenean foreland basin infill, especially for short-term events like the Cardona salt deposition, we do not include them in the presented backstripping analysis. First-order cycle sea level decreases regularly from *c.* 220 m at the base of the Eocene to *c.* 190 m at the top of the Eocene (Vail *et al.* 1977; Haq *et al.* 1987). The Beuda and particularly the Cardona evaporitic intervals approximately correspond to marked sea-level falls (–100 m) in the published curve (as noted in Burbank *et al.* 1992*a*), and may introduce additional uncertainties to the subsidence analysis. The Beuda and Cardona evaporitic successions are characterized by shallowing-upward sequences culminating in subaerial exposure at the top of the unit in the case of the Beuda succession (Ortí *et al.* 1988). The decreasing palaeobathymetry related to these units might reflect the variation of the ratio between tectonic subsidence and variations in sea-level. If we hold the tectonic subsidence constant for these short intervals of time, then the shallowing-upward sequence would be produced only by a sea-level drop. However, if the shallowing-upward palaeobathymetry observed in the Beuda unit is related to a sea-level fall, then the tectonic uplift associated with this evaporitic unit would be apparent (see Gombrèn subsidence curve in Fig. 8).

Apparently abrupt slope changes in the subsidence curves are primarily artifacts of the calculation technique in which constant rates are calculated between dated endpoints that are widely separated in time. In addition use of local Airy isostasy tends to amplify apparent rate changes that would be more subdued if lateral flexural strength were taken into account. These abrupt changes have no geological significance as can be deduced by the widespread gradational contacts between different depositional units. The uppermost interval of most of the analysed sections corresponds to continental deposits that have been partially eroded, such as the Bellmunt Fm in the Gombrèn section and the Solsona Fm south of the Vallfogona thrust. Subsidence curves for these uppermost segments of the sections have been determined using marine equations for water-loaded crust and assuming the extrapolated age of the top of each section represents its final stage of deposition (Figs 8 & 9). Table 2 lists the input parameters (age of the top of the selected interval, present thickness, final density of the whole interval, and bathymetry) and results (total and tectonic subsidence and decompacted thickness) for each of the analysed sections.

Subsidence and tectonics: geohistory

The subsidence curves display a typical foreland basin convex-up shape with an inflection point dating the onset of the most intense period of tectonic subsidence (Figs 8 & 9). The Gombrèn section displays the first inflection point at 55.9 Ma coinciding with the onset of marine conditions within the basin after a long period of time characterized by widespread continental Palaeocene deposition (Figs 4 & 8). The second inflection point, at 50.7 Ma coincides with the basal part of the second depositional cycle represented by marls and calcareous marls of the Armàncies Fm. During deposition of siliciclastic turbidites of the Campdevànol Fm, there is a marked decrease in tectonic subsidence values (Figs 8 & 9). During Beuda deposition, the tectonic subsidence pattern starts to show an upward vector of motion that is distinctive of the latest evolution of the Ripoll basin as a piggy-back basin during the Bellmunt Fm fluvial deposition. Nevertheless, as has been noted previously, a sea-level drop of *c.* 100 m would be sufficient to invert the calculated upward disposition of the total subsidence curve during the Beuda interval.

The Jabalí and Puig-reig subsidence curves show the southward migration of their first inflection point. In the Jabalí section the first inflection point corresponding to a considerable increase in tectonic subsidence is located around 46.26 Ma, several millions of years later than the Gombrèn inflection points. However, the most important inflection point in this curve corresponds to 43 Ma as well as in the Puig-reig

Table 2. *List of stratigraphic unit age, present thickness, final density and bathymetry for each of the analysed intervals. Total and tectonic subsidence as well as decompacted thickness for each sedimentary interval of the analysed sections are given.*

	Age (Ma)	Present thickness (m)	Density (g cm^{-3})	Bathymetry min – max (m)		Total subsidence (m)	Tecctonic (m)	Decompacted thickness (m)							
Gombrén								Ma:	55.90	52.05	50.69	49.36	46.85	46.18	45.82	42.65
Bellmunt	42.65	1203.4	2.56	–100	0	4430.6	2053.9								–	1203.4
Coubet	45.82	126.8	2.52	0	30	3741.7	1829.7								195.7	126.8
Beuda	46.18	170.0	2.39	0	100	3702.9	1844.7						–	278.8	244.6	170.0
Campdevánol	46.85	723.2	2.54	100	300	3721.7	1945.5					–	1064.3	940.1	895.4	723.2
Armáncies	49.36	1076.6	2.52	15	300	3097.4	1704.2				–	1624.0	1212.9	1197.7	1168.5	1076.6
Corones	50.69	225.6	2.60	–5	15	1757.8	995.7			–	423.6	259.4	241.4	238.6	235.9	225.6
Sagnari	52.05	465.0	2.59	0	75	1555.0	934.8		–	857.1	705.0	520.4	491.1	485.7	480.3	465.0
Paleocene	55.90	490.0	2.59	–100	0	793.9	478.4		843.9	660.4	624.2	536.1	512.0	512.0	506.3	490.0
Basement	65.00	4480.6				0.0	0.0		843.9	1517.5	1752.8	2939.9	3251.7	3652.9	3726.7	4480.6
Jabalí								Ma:	49.0	46.26	43.0	41.5	40.0	36.81	33.77	
Solsona	33.77	698.0	2.52	–100	0	3650.0	1767.8							–	698.0	
Igualada-Tossa	36.81	1410.0	2.53	30	150	3364.3	1727.1						–	1621.5	1410.0	
Folgueroles	40.0	155.0	2.59	100	150	2173.1	1184.7					–	227.9	166.1	155.0	
Banyoles	41.5	580.0	2.55	50	100	2004.7	1090.2				–	914.6	834.4	609.7	580.0	
Tavertet	43.0	417.0	2.65	10	30	1286.8	697.5			–	699.9	515.8	496.2	430.8	417.0	
Penya	46.26	143.0	2.72	10	15	726.6	419.2		–	259.0	190.7	163.4	161.5	146.0	143.0	
Cadi	49.0	297.0	2.68	0	30	528.0	322.8		513.0	455.1	376.2	335.9	328.1	300.2	297.0	
Basement	55.90	3700.0				0.0	0.0		513.0	714.1	1266.8	1929.7	2048.1	3274.3	3700.0	
Puig-Reig								Ma:	49.0	46.26	43.0	41.5	40.0	36.81	34.36	
Solsonia	34.36	563.2	2.54	–100	0	3175.7	1604.9							–	563.2	
Igualada-Tossa	36.81	1662.8	2.44	30	150	3013.3	1640.6							1896.6	1662.8	
Folgueroles	40.0	97.5	2.54	100	150	1556.7	940.4						175.9	101.1	97.5	
Banyoles	41.5	218.0	2.52	50	100	1401.4	841.9				–	402.8	363.3	226.0	218.0	
Tavertet	43.0	127.0	2.64	10	30	1078.6	641.3			–	226.6	183.4	175.1	129.9	127.0	
Penya	46.26	96.7	2.67	10	15	925.6	572.3		–	177.9	156.1	132.8	127.1	98.9	96.7	
Cadi	49.0	460.5	2.59	0	30	820.9	530.1		805.9	735.2	675.9	607.3	580.2	470.8	460.5	
Basement	55.90	3225.7				0.0	0.0		805.9	913.1	1058.6	1326.3	1431.6	2923.3	3225.7	

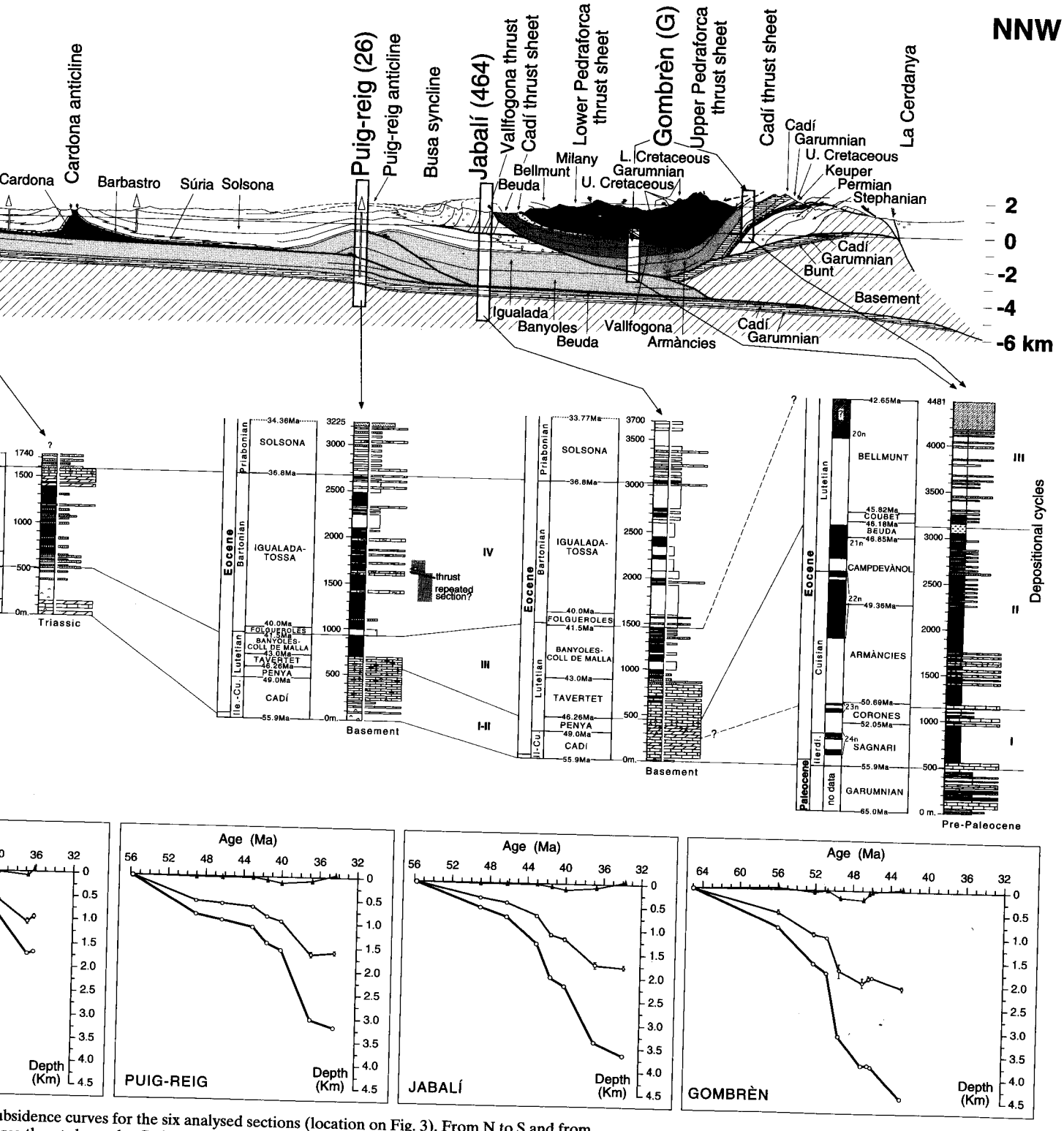

ubsidence curves for the six analysed sections (location on Fig. 3). From N to S and from
rca thrust sheet, the Cadí thrust sheet (with the Gombrèn section), and the deformed fore-
Coastal Ranges. These are overprinted by normal faulting related to the uppermost Oligo-
the Gombrèn section to show the onset of important tectonic subsidence coeval with the
tectonic duplication by thrusting.

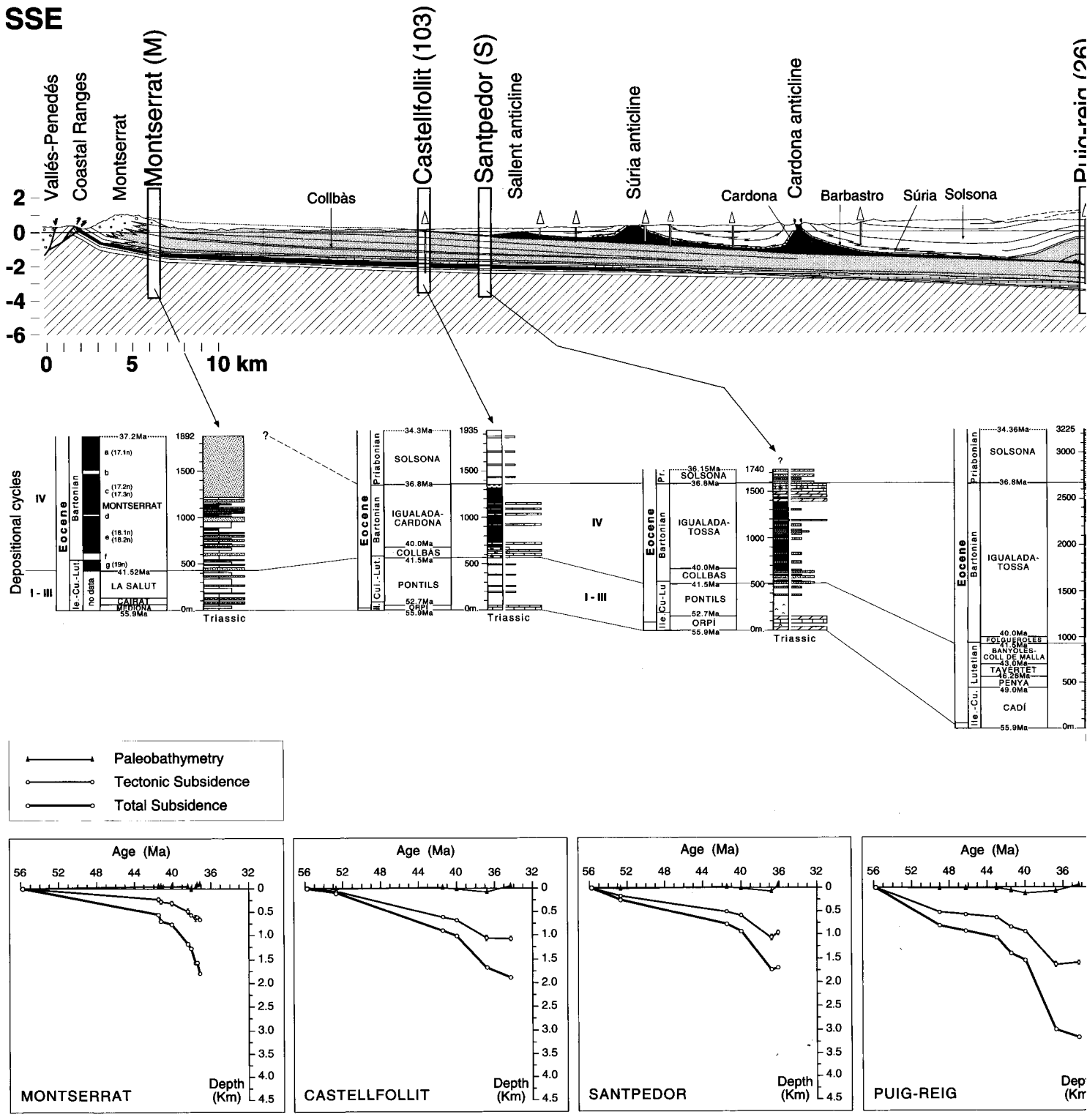

Fig. 8. Regional balanced geological cross-section, simplified stratigraphic columns, depositional cycles and subsidence curves for the six analysed sections (loca the upper to the lower structural level, the section shows the upper Pedraforca thrust sheet, the lower Pedraforca thrust sheet, the Cadí thrust sheet (with the G land basin (with the rest of analysed sections). The southern margin of the basin is constituted by the Catalan Coastal Ranges. These are overprinted by normal cene–Miocene València Trough opening. Paleocene deposits have been included in the subsidence analysis of the Gombrèn section to show the onset of import onset of marine marly Sagnari Fm deposits into the basin. Shading in the Puig-reig section shows the potential tectonic duplication by thrusting.

Santpedor								Ma:	52.7	41.5	40.0	36.81	36.15			
Solsona	36.15	150.0	2.53	−100	0	1690.0	963.7					–	150.0			
Igualada-Tossa	36.81	920.0	2.44	30	150	1742.4	1067.1				–	967.6	920.0			
Collbas	40.0	160.0	2.58	0	50	926.9	601.4			–	212.0	162.5	160.0			
Pontils	41.5	360.0	2.52	−10	0	762.8	509.1		–	580.9	511.2	370.4	360.0			
Orpí	52.7	150.0	2.61	0	30	262.9	177.8		247.9	186.9	178.7	151.9	150.0			
Basement	55.90	1740.0				0.0	0.0		247.9	767.8	901.9	1652.4	1740.0			
Castellfollit								Ma:	52.7	41.5	40.0	36.81	34.31			
Solsona	34.31	574.0	2.52	−100	0	1885.0	1077.4					–	574.0			
Igualada–Cardona	36.81	683.0	2.41	30	150	1687.7	1062.5					860.1	683.0			
Collbas	40.0	108.0	2.52	0	50	1016.2	675.7			–	177.6	119.3	108.0			
Pontils	41.5	521.0	2.53	−10	0	891.5	603.1		–	838.1	756.0	567.0	521.0			
Orpí	52.7	49.0	2.65	0	30	98.6	68.1		83.6	58.4	57.6	51.3	49.0			
Basement	53.90	1935.0				0.0	0.0		83.6	896.5	991.2	1597.7	1935.0			
Montserrat								Ma:	41.52	41.25	40.13	38.42	38.11	37.60	37.47	37.2
(17.1n)	37.2	370.0	2.60	−130	−60	1796.8	661.7								–	370.0
	37.47	50.0	2.60	−100	−60	1552.4	592.7								56.0	50.0
(17.2.3n)	37.60	432.5	2.58	−100	30	1560.7	622.6						–	482.4	473.3	432.5
	38.11	28.0	2.55	20	30	1268.5	556.3					–	38.4	30.9	30.4	28.0
(1.8n)	38.42	399.5	2.57	−100	20	1168.9	476.6				–	501.3	501.3	433.4	433.4	399.5
	40.13	68.0	2.57	−100	0	752.6	305.1			–	95.5	81.6	80.1	72.4	71.2	68.0
(1.9n)	41.25	120.0	2.58	−100	0	684.3	279.3		–	166.5	160.0	140.7	138.3	127.5	125.5	120.0
Mediona-La-Salut	41.52	423.8	2.57	−100	0	551.8	225.4		601.8	567.7	547.1	485.3	485.3	449.1	442.5	423.8
Basement	55.90	1891.8				0.0	0.0		601.8	734.2	802.6	1208.9	1243.4	1595.7	1623.3	1891.8

Montserrat section calculated with continental and marine equations (shaded intervals). The ages of the continental Orpí and Pontils Fms are fixed although they could become younger to the south as discussed in text.

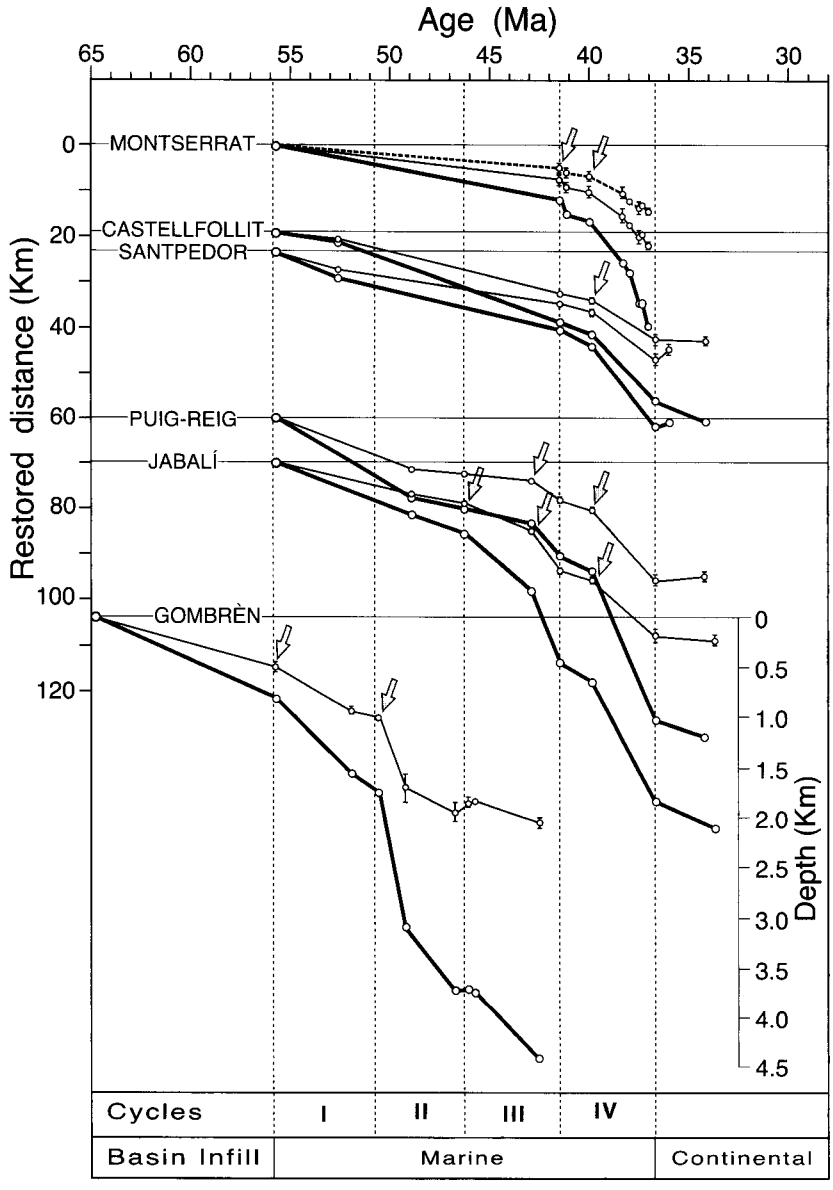

Fig. 9. Plot of total (lower and thick black lines of each curve) and tectonic (upper lines of each curve) subsidence versus time. The position of each profile is restored to its pre-thrusting position according to the restored version of the cross-section shown in Fig. 8 (Vergés 1993; Vergés & Burbank 1996). As in Fig. 8, tectonic subsidence curves are calculated for marine equations using the age of the uppermost strata preserved in the section as a final age-value of the analysis. The Montserrat curve shows results using both continental (dashed thin black line) and marine equations (thin black line) for the sake of comparison. Arrows show the position of the inflection points related to the initiation of subsidence events. From Gombrèn to Montserrat, the migration of the flexural wave occurred at a rate of *c.* 10 mm a^{-1} throughout 104 km of the southern Pyrenean foreland basin.

section. This period of strong subsidence corresponds to deposition of marly deposits of Banyoles Fm. The younger segments of these curves display smaller amounts and rates of tectonic subsidence during deposition of alluvial and fluvial deposits corresponding to the Solsona

Fm. To the south of these two wells, the Santpedor and Castellfollit subsidence curves show their first and unique inflection point at 40.0 Ma as well as the Montserrat curve. However, the Montserrat section shows a previous and very rapid period of tectonic subsidence at 41.5 Ma at the base of the conglomeratic Montserrat Fm that contains growth strata geometries proving its unambiguous syntectonic character (López-Blanco 1993). Although time control in the Santpedor and Castellfollit sections is not so well constrained as it is in the Montserrat section, the short-term high-rate of tectonic subsidence determined at 41.5 Ma suggests that Catalan Coastal Ranges influenced subsidence in the southern segment of the Ebro foreland basin. The product of this tectonic activity in both margins of the Ebro basin during middle Eocene time resulted in a double flexure as observed in cross-section (Fig. 8) and two opposite prograding deltaic clastic wedges related to the active margins of the foreland basin (Fig. 4).

Based on the combination of balanced and restored cross-sections and palinspastic maps (Vergés 1993; Vergés & Burbank 1996), Fig. 9 shows the tectonic subsidence curves in a restored position with the Montserrat section used as a pin point. This restoration permits calculation of the rate of southward migration of the position of the first inflection point and thus the onset of the tectonic subsidence within different segments of the Ebro foreland basin. The rate of flexural wave migration across 104 km of basin width (from Gombrèn to Montserrat sections) is *c.* 10 mm a^{-1}. At the same time along the southern margin of the basin, the shallow-water carbonate platforms (as imaged in seismic line S-7, Fig. 6) migrate at the same velocity to maintain the particular bathymetric conditions required for their growth (backstepping foreland carbonate ramps; Dorobek 1995).

Subsidence in the foreland basins is coupled to the emplacement of tectonic loads within the orogen (Price 1973; Beaumont 1981; Jordan 1981). The parallel trend of the subsidence transect and the Pyrenean tectonic transport permits investigation of a direct relationship between tectonics and subsidence. The ages of the emplacement of southeastern Pyrenean thrust sheets have been previously documented based on cross-cutting relationships between thrusts and syn- and post-thrusting sediments dated by classical methods (Puigdefàbregas *et al.* 1986; Vergés & Martínez 1988). A more complete approach on the timing of thrusting was presented by Burbank *et al.* (1992*a,b*), using both magnetostratigraphy and subsidence analysis. Thrust emplacement ages were recalibrated for the Cande & Kent (1992) global polarity time scale in Vergés & Burbank (1996), whereas the links between cover and basement thrust sheets as well as a compilation of ages of thrusting along a complete N–S crustal transect crossing the Pyrenees was presented in Vergés *et al.* (1995). This subsidence analysis represents a complementary and independent constraint to date thrust development and will allow us to determine better the onset of different events of thrust, the geometry and rates of tectonic subsidence, and the rate of its propagation across the foreland (Figs 9 & 10).

The strong subsidence events determined in the northernmost Gombrèn section, cropping out in the northern flank of the Ripoll syncline, reflect the emplacement of the Pedraforca thrust sheets (the upper southern Pyrenean thrust sheets: Muñoz *et al.* 1986). Tectonic subsidence starts at the base of the first depositional cycle (55.9 Ma) and strongly increases at the base of the second cycle (50.69 Ma). The parallel increase of the rate of tectonic subsidence, to 0.53 mm a^{-1}, is related to the southward emplacement of the Pedraforca cover thrust sheets and Nogueres basement unit. The submarine and rapid emplacement of the front of these tectonic units is demonstrated by syntectonic sediments containing blocks and olistolites derived from the front of the overriding thrust sheets (Vergés & Martínez 1988) and palinspastic maps (Vergés & Burbank 1996). At basin-scale, relatively deep marine sedimentation (Armàncies and Campdevànol Fms), recording the underfilled stage of the foreland basin, coincides with the period marked by highest rates of tectonic shortening (> 4 mm a^{-1}), rapid thrust-front advance and a first stage of Pyrenean orogenic growth characterized by a relatively low topographic relief (Vergés *et al.* 1995). This parallelism of underfilled basin conditions and high rates of tectonic advance has been observed in the Swiss Molasse basin (Allen *et al.* 1991) and simulated with foreland basin modelling (Flemings & Jordan 1989; Sinclair *et al.* 1991).

Decreasing tectonic subsidence values and rates (0.10 mm a^{-1}) recorded during the turbiditic deposition of the Campdevànol Fm between 49.36 and 46.85 Ma, are related in this work to the initial deformation within the south Pyrenean foreland basin before its partition into a transported Ripoll piggyback basin to the north and a major foreland basin to the south. This deformation was achieved by a combination of layer parallel shortening, folding and thrusting probably related to the forelandward propagation of the Vallfogona thrust across foreland deposits that triggered the large

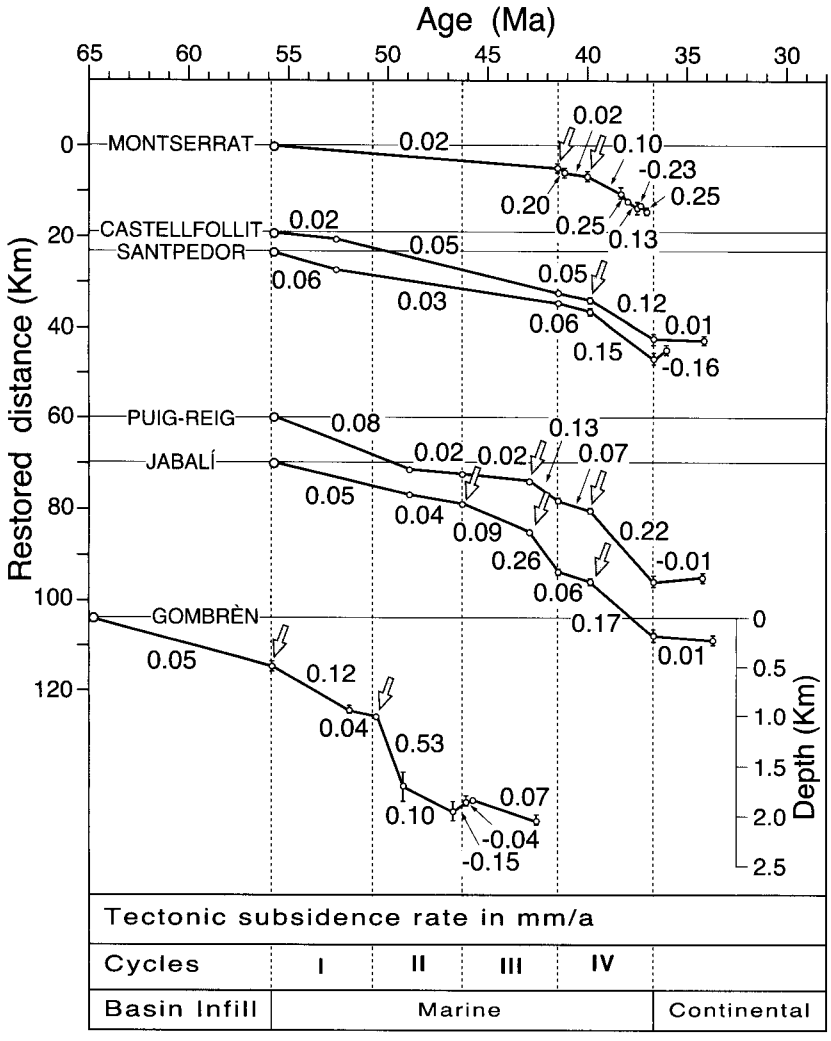

Fig. 10. Plot of tectonic subsidence rates in mm a^{-1} using reference time slices. The position of each of the profiles is restored to the pre-thrusting position as in Fig. 9. Maximum subsidence rates are as high as 0.53 mm a^{-1} (from 50.69–49.36 Ma) in the Ripoll basin. These rates decrease, migrate and become younger toward the foreland ranging from 0.26 mm a^{-1} (43–41.5 Ma at 34 km away of the Vallfogona thrust) to 0.22 mm a^{-1} (40.0–36.8 Ma at 44 km away of the same position) to 0.15 mm a^{-1} (same age at 80 km away of the Vallfogona thrust).

number of slumped deposits found within the turbidites of the Campdevànol Fm, after 49.36 Ma. Following this interpretation, the deformation within the Ripoll basin started before the final emplacement and fossilization of the lower Pedraforca thrust sheets at around 47 Ma, as determined by cross-cutting relationships (Martínez *et al.* 1988; Vergés *et al.* 1994) and middle Lutetian basin reconstruction (Vergés *et al.* 1995).

The general decrease of tectonic subsidence (0.07 mm a^{-1}) related to the fluvial deposition of the Bellmunt Fm is attributed to the onset of upward motion of the Ripoll basin on top of the Vallfogona thrust ramp at 42.65 Ma. To the south, the Jabalí section records a first pulse of tectonic subsidence with rates of almost 0.1 mm a^{-1} at 46.26 Ma and a stronger pulse with rates of 0.26 mm a^{-1} at 43 Ma that is also recorded in the Puig-reig section (0.13 mm a^{-1}). Tectonic subsidence registered in Jabalí and Puig-reig sections was persistent reaching values of 0.17 and 0.22 mm a^{-1} from 40.0 to 36.81 Ma, although the last value could be overestimated

because tectonic duplication is inferred underneath the Puig-reig anticline. These events of subsidence are interpreted to result from the emplacement of the Cadí thrust sheet and attached Orri basement unit, coincident with deformation of syntectonic sediments located in the footwall of the Vallfogona thrust, that took place from at least 42 Ma to the late Eocene–early Oligocene time (Burbank *et al.* 1992*a*; Mató *et al.* 1994). Deformation within the footwall of the Vallfogona thrust is widely recognized in both geological maps and seismic lines. The geological map of Berga shows different stratigraphic units bounded by unconformities and affected by different sets of folds and thrusts. This is exemplified by unconformities that seal older sets of folds and are folded by a new group of tectonic structures (Mató *et al.* 1994). According to Mató *et al.* (1994), these growth strata units correspond to the fourth depositional cycle. South of the Vallfogona thrust, the western termination of the Bellmunt anticline is also coeval with the fourth depositional cycle, starting after 41.5 Ma (Fig. 7). Deformation of the foreland-basin strata above a regional detachment level is associated with emplacement of the basement Rialp unit after 37 Ma (Vergés *et al.* 1995) and to the activity as an out-of-sequence fault of the Ribes–Camprodon thrust (Burbank *et al.* 1992*a*).

Abrupt increase of tectonic subsidence at 41.5 Ma in the southernmost margin of the Ebro basin is linked to the onset of tectonic activity related to the front of the Catalan Coastal Ranges involving basement rocks (López-Blanco *et al.* in press). It should be noted that this increase of tectonic subsidence is slightly recorded in Castellfollit and Santpedor sections, but not in the more northern Puig-reig and Jabalí ones. This differential subsidence response agrees with the doubly flexed geometry of the basin determined in the regional cross-section (Vergés & Burbank 1996; Fig. 8). The onset of strong deformation along the southern margin of the basin is at least partly coeval with the forelandward propagation of deformation in the Ebro basin, suggesting that the initial tectonic activity of the deep-seated thrust of the front of the Catalan Coastal Ranges could be triggered by the transmission of stresses throughout the upper crustal levels of the Iberian plate from its northern margin underneath the Pyrenees.

All the curves within the Ebro basin show either decreasing rates of tectonic subsidence or tectonic uplift during the continental deposition of the Solsona Fm following the marine Cardona salt deposition at 36.8 Ma. Post-thrusting evolution of the Ebro basin is important to complete the history of vertical motions of any of the sections that are located south of the Vallfogona thrust and which are affected by tectonic uplift related to the extensional fault system developed during the opening of the València Trough starting at *c.* 25 Ma (uppermost Oligocene–lower Miocene; Bartrina *et al.* 1992) but probably effective at 16 Ma coinciding with increasing sediment accumulations in the València Trough continental platform (Roca 1992).

Geohistory of Gombrèn and Jabalí sections across the Vallfogona thrust shows distinctive vertical motions, especially after deposition of relative deep-marine, marly Armàncies and turbiditic Campdevànol Fms (Fig. 11). Development of the Ripoll syncline was coeval with fluvial Bellmunt Fm deposition. Uppermost flat-lying conglomerates display an angular unconformity with the lower Eocene marine series cropping out in the northern flank of the Ripoll syncline and permit quantification of synthrusting rock uplift and denudation achieved during Oligocene times (Vergés *et al.* 1995). Using a linear geothermal gradient of 30°C km^{-1} that is slightly high for foreland basins, it is possible to estimate the palaeotemperature of the section during its burial history (Fig. 11). This simple correlation indicates that the lower part of the Armàncies Fm was buried to 3250 m reaching a maximum temperature of *c.* 100°C. These results are in agreement with determinations of Tmax of the lower part of the Armàncies Fm source rock indicating that it moved through the upper part of the oil window area (Permanyer *et al.* 1988; Clavell 1992). The comparison of geohistories across the Vallfogona thrust shows opposite vertical motions. The Gombrèn geohistory indicates a general uplift event during the southern transport of the Cadí thrust sheet on top of the Vallfogona thrust whereas to the south of this thrust, the Jabalí geohistory shows pervasive subsidence to the end of Solsona Fm deposition. Using the same geothermal gradient of 30°C km^{-1} the base of the section reached 3650 m of palaeoburial depth corresponding to 110°C of palaeotemperature.

Discussion

Subsidence analysis

The subsidence analysis presented in this study is carried out along a N–S transect, parallel to the tectonic transport direction. Although we do not incorporate the flexural component of the plate, the calculated amounts and rates at which the foreland basin has subsided due to the

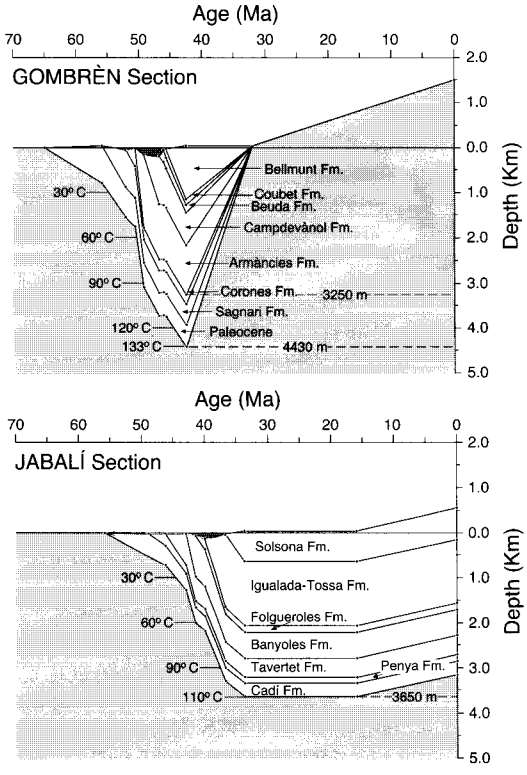

Fig. 11. Geohistory of the Gombrèn and Jabalí sections located in both sides of the Vallfogona thrust. An assumed (slightly high) geothermal gradient of 30°C km^{-1} is plotted to show palaeotemperatures during burial. Geochemical data from the lower part of the source rock Armàncies Fm indicate that it passed through the upper part of the oil window whereas the presented geohistory suggests that it did not. The most convincing explanation is that a part of the Bellmunt Fm has been eroded after the end of deposition in mid- Eocene times. Uplift of the northern flank of the Ripoll syncline occurred during thrusting and before the deposition of continental Tertiary flat-lying conglomerates that unconformably overlie the south dipping lower and middle Eocene series. The Jabalí geohistory shows a younger age for the onset of subsidence, a renewed subsidence event during uplift in the Gombrèn section and widespread subsidence to the end of deposition.

Pyrenean tectonic loading are adequate to show the relative vertical motions throughout the basin. Each of the studied sections shows a convex-up subsidence curve with one or two intervals of rapid tectonic subsidence marked by inflection points. The almost flat segment of the curve before the first inflection point represents a period of slow sedimentation, hiatus or even erosion that has not been corrected due to the lack of accurate information. If our interpretation of seismic line S-7 is correct (Fig. 6), in which the shallow marine platforms (Penya and Tavertet Fms) migrate to the south with basal and top boundaries also becoming younger to the south, then the nearly flat segments of the subsidence curve would show a different geometry than that indicated by the subsidence curve: the initial long segment of the curve would be shorter and would start later.

In the southernmost sections analysed in this work, the thicknesses have not been corrected for overburden due to post-thrusting eroded continental deposits. Additional depositional loads in these sections can decrease or even reverse the upward tendency of the upper segment of the tectonic subsidence curve as shown in the next section.

Post-thrusting Ebro foreland basin history

The Post-thrusting history of the Ebro basin is more difficult to unravel because it has been characterized by erosion, especially in its southeastern margin. Uplift and erosion of the southern part of the basin is related to the development of onshore normal faults oriented roughly parallel to the coast (Fig. 3) and linked to the development of the València Trough (Lewis *et al.* 1996), starting in latest Oligocene–Early Miocene time. In order to estimate the amount of denudation related to the southeastern segment of the Ebro basin, two coals (five specimens) from Santpedor and Calaf (see location in Fig. 3) have been studied to determine the vitrinite reflectance expressed as mean values of random reflectance (R_m). These samples can be projected to near the top of the Castellfollit oil-well in cross-section. The two coals furnished R_m values between 0.44% and 0.48% with deviations of 0.05. However, in this study we compare these results with R_m values provided by oil-wells more to the north. In the studied transect, the Puig-reig oil-well shows R_m values of 0.45% from 1.45 to 1.9 km of depth (Clavell 1992) and the Jabalí one at 1.65 km. However, the best data come from the Basella oil-well, which cuts a thick and complete Solsona Fm continental succession (located westward of the study transect; see oil-well 96 in Fig. 3). This oil-well shows R_m values of 0.45% at a depth of 2.9 km (Clavell 1992). The correspondence between R_m values and burial depths observed, especially in the Basella oil-well, is consistent with estimations of paleotemperatures and palaeodepths calculated using standard conversion methods and thus corroborating the interpretation that observed depths of 2.9 km

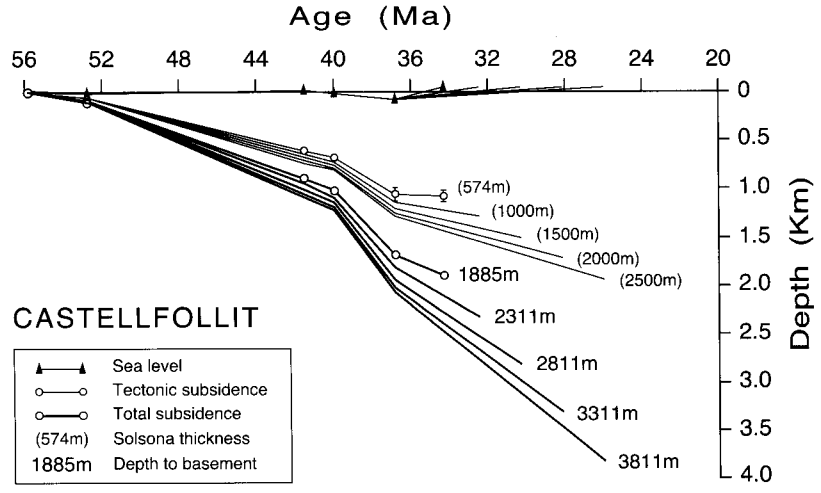

Fig. 12. Interpretative subsidence analysis for the Castellfollit section assuming extra amounts of sediments on top of the section to account for potential erosion since the end of deposition. These extra amounts are slices of 500 m up to a total Solsona Fm of 2500 m (see discussion in the text). The subsidence curves are calculated using marine equations, the age of the uppermost strata preserved in the section as a final age-value of the analysis and a mean palaeobathymetry for the extra continental deposits of 50 m above sea level.

correspond to maximum burial depths. According to this correlation between R_m values and observed burial depths, the calculated R_m of 0.44–0.48% located at the surface strongly suggests a palaeoburial depth of 2–3 km for these sediments. The correlation of R_m values along the studied N–S transect implies differential denudation south of the Vallfogona thrust that increases to a maximum close to the Catalan Coastal margin.

To test the effects in the subsidence analysis of these inferred extra amounts of material in the southern side of the Ebro foreland basin, we added slices of 500 m of strata on top of the Castellfollit section to up to 2000 m (Fig. 12). The subsidence analysis is made using marine equations. These calculations assume a constant negative bathymetry above sea-level between 0 and −100 m for the upper slice, post-sedimentation uplift to the present position with concomitant erosion, and ages of the topmost strata as estimated by extrapolation. The age of the topmost part of each of these slices has been calculated using mean values of sediment accumulation rate of 0.23 mm a^{-1} as described previously. The age of the top of the total 2500 m of Solsona Fm continental fluvial strata would correspond to the Late Oligocene (*c.* 26 Ma). This extrapolated age agrees with the well-determined upper Oligocene age reported from equivalent strata attached to the Pyrenean front, cropping out 40 km to the northwest in Artesa del Segre (Meigs *et al.* 1996; see location in Fig. 3).

The results of these analysis show that independent of the amount of material added in the top of the Solsona strata, the tectonic subsidence curves for the underlying intervals show little variation. Tectonic subsidence curve corresponding to 574 m (the present Solsona Fm thickness) show almost a flat trend whereas curves corresponding to 1000, 1500, 2000 and 2500 m show downward trend during Solsona deposition. The total subsidence increases as the thickness of the upper interval increases from 1885 m for the top of basement at the end of deposition of 574 m of Solsona Fm to 3811 m at the end of the deposition of 2500 m of Solsona Fm and material located on top of the present section (at 574 m), cropping out today at 729 m above sea-level would be located at a minimum depth of 1.9 km at the end of Solsona Fm deposition (Fig. 12).

Since the palaeoaltitude of the top of the additional Solsona Fm deposits has been fixed at 50 m above sea-level, the removal of almost 2000 m of material would not increase this altitude to the present 729 m by simple isostatic rebound. Only with palaeoaltitudes of slightly over 1000 m would be possible to reach the present altitude due to erosionally driven isostasy. Because it is unlikely that the basin was ever filled to this altitude, the present elevation of the outcrops of Solsona strata suggests significant tectonically

driven uplift following deposition. This analysis shows the potential behavior of the foreland basin filled with additional material that presumably has been denuded since the end of deposition in the Ebro basin.

Subsidence and third order depositional cycles

Rapid progradations of continental clastic deposits covering a large part of foreland basins have been associated with periods of tectonic quiescence (Heller *et al.* 1988). In this model, during periods of thrusting, clastic sediments are trapped in rapidly subsiding troughs close to the thrust front. During tectonic quiescence, isostatic flexural rebound triggers erosion in the mountain range and the products prograde into the uplifting basin and thus depositing thin sheets of coarse material unconformably overlying syntectonic series. Using a dynamic model, Jordan & Flemings (1991) reproduce transgressive–regressive third-order marine–continental sedimentary packages by using repeated periods of tectonic activity and quiescence. They reproduce a complete depositional cycle with 4 Ma of thrusting followed by 2 Ma of tectonic quiescence, a result that can not be attained with sea-level variations alone. However, these models also utilize a simple deformation front defined by a single thrust.

According to the above mentioned models and using the second depositional cycle as an example, the talus marls (Armàncies Fm) and siliciclastic turbidites (Campdevànol Fm) would be related to the emplacement of hinterland tectonic loads, whereas the deposition of evaporites (Beuda Fm) would be related to tectonic quiescence. However, widespread syndepositional deformation together with intercalated olistostromes and slumps indicate a roughly continuous forelandward displacement of the Pedraforca–Nogueres thrust sheet during this entire interval. The final emplacement of this large thrust sheet took place on top of the evaporites of the Beuda Fm. According to these data it seems that the transgressive–regressive depositional cycle could be linked to a different mechanism of formation than that proposed in the activity–quiescence models.

The fact that folding and thrusting occurs during the foreland infill has been widely recognized (e.g. Ricci Luchi 1986). The effect of this syn-depositional faulting in the sedimentary infill of a foreland basin has been kinematically modeled using simple cases (e.g. Zoetemeijer *et al.* 1992; Peper 1993). However, the frontal regions of the eastern Pyrenees foreland basin show distributed deformation affecting large areas of syn-tectonic strata. This deformation was produced above detachment levels that could transfer deformation very efficiently. The thickening of the sedimentary pile by layer-parallel shortening, thrusting and folding could be responsible for simultaneous decrease of the available space in the basin (Fig. 13). In such a case, the rapidity of this thickening process would depend on the efficiency with which the detachment level propagates the deformation far away from the previous deformation front and the velocity at which this process could take place.

Furthermore, overthickened depositional units give overestimated amounts and rates of subsidence, depending on the lithologies. Several locations of the apparently non-deformed eastern Ebro foreland basin display tectonic thickening above 20% (Casas *et al.* 1996). We agree with DeCelles & Giles (1996) that distinction of different segments of foreland basins as well as the controls on particle paths during foreland basin evolution are important to understanding and interpreting subsidence analysis.

Comparison with other European foreland basins

Tertiary Western European foreland basins are relatively complicated, commonly partitioned,

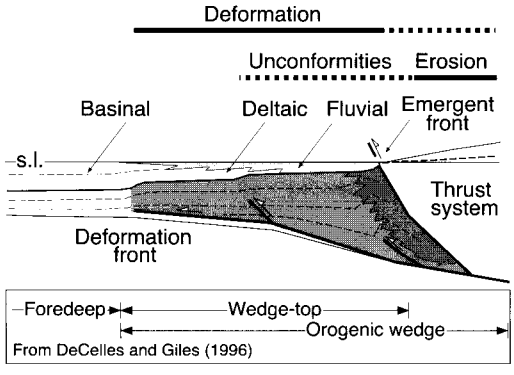

Fig. 13. Cartoon showing the geometry, sedimentary facies and deformation distribution within a stratigraphic unit affected by an advancing buried deformation front. Tectonic thickening of the strata located above a detachment level (shaded) produces a decrease of available space on this segment of the basin. Efficient detachment levels within the basin and concomitant overthickening of large segments of the basin could be responsible for the transgressive part of a third order depositional cycles (at least partially).

and limited in size due to the complex interaction between small plates and rigid basement blocks that controls the geometry of both foreland basins and mountain ranges (Fig. 2). These foreland basins are located between the convergent African and European large-scale plates and developed after the collision of continental blocks moving at relatively low rates. The history of these basins was similar and partially synchronous, with depocentres migrating at the front of forelandward propagating thrusts. The post-foreland basin histories are different depending on the final geodynamic evolution of the basin, and they vary from uplifted basins like the southeastern Pyrenees and Swiss Molasse basins to more or less preserved basins like the northwestern Pyrenean and German Molasse basins.

The available information on transects similarly located with respect to the front of thrusting permits the comparison of subsidence results among our study area and the Aquitaine basin, the Swiss Molasse basin and the German Molasse basin (Table 3).

The Tertiary development of the Aquitaine basin (Fig. 2), formed on top of Mesozoic rifted European plate, was produced by the inversion of Mesozoic extensional structures toward the north (e.g. Daignieres *et al.* 1994). A local isostatic backstripping analysis from ten oil-wells has been determined by Dubarry (1988). Her results show an increasing subsidence rate starting at around 60 Ma (Thanetian) and culminating at 54–53 Ma (early Ypresian) with rates of tectonic subsidence ranging 0.16–0.2 mm a^{-1} (Dubarry 1988). This rapid phase of subsidence coincided with the emplacement of northern Pyrenean thrust sheets. The end of the rapid subsidence was marked by a progressive decrease of bathymetry at the beginning of continental deposition a few million years later (Table 3). More regional studies suggest that the end of subsidence migrated toward the west, where it was greatest during Oligocene times in positions close to the present boundary of the Bay of Biscay (Desegaulx & Brunet 1990). The control of previous rifted margins also influenced the subsidence results in the Aquitaine basin (Desegaulx *et al.* 1991).

Located in front of the emergent Alpine thrust front, the Swiss Molasse basin is in part located on top of the detached fold-and-thrust system of the Jura Mountains, although older foreland basin deposits are incorporated in the Alpine thrust system. Analysing the results from the Swiss Molasse basin deposits adjacent to the Alps, we see a comparable subsidence signature to that of the southern Pyrenean foreland. Homewood *et al.* (1986), using an Airy model of compensation, determined tectonic subsidence rates similar to the studied Spanish example. These were 0.1 mm a^{-1} at the front of the mountains and 0.06 mm a^{-1} in the distal parts of the basin. The rate of migration of depositional depocentres was 9 mm a^{-1} during Oligocene times but decreased to 2 mm a^{-1} during Miocene times (Homewood *et al.* 1986).

To the east, the German Molasse basin seems to be largely undisturbed, but is slightly deformed close to the Alpine front. In the German Molasse basin a flexural backstripping analysis defines rates of tectonic subsidence between 43 and 23 Ma. The rates were as high as 0.2–0.6 mm a^{-1} in adjacent to the front (the highest is 0.9 mm a^{-1} during 27–26 Ma), and 0.08–0.3 mm a^{-1}, 60 km away from the front positions, using an effective elastic thickness of 48 km (Jin 1995).

Conclusions

The general pattern of subsidence curves along a N–S transect crossing the South Pyrenean foreland basin shows a coupling between thrusting and flexural response in the basin which produces propagation of depocenters and sedimentary cycles toward the foreland side of the underthrust Iberian plate.

The subsidence curves of the sections analysed in this work show the typical convex-up signature of foreland basins. The Gombrèn section represents an early foreland basin (55.9 Ma to at least 42.65 Ma) that has been transported as a piggyback basin by the Vallfogona thrust starting at around 47 Ma although internal deformation could start 2 Ma earlier (first and second depositional cycles). Maximum rates of tectonic subsidence are 0.53 mm a^{-1} in the Gombrèn section. This relatively short interval of rapid subsidence (50.69–49.36 Ma) was characterized by the deposition of relatively deep marine marls intercalated with slope megabreccia deposits (Armàncies Fm), linked to several northward progradations of shallow-marine carbonate platforms. South of the Vallfogona thrust, maximum rates of tectonic subsidence are around 0.26 mm a^{-1} in the center and southern margin of the Ebro basin. The flexural wave propagated at *c.* 10 mm a^{-1} across the basin. At this rate, the propagation of the flexural wave took only 10–11 Ma to affect the whole foreland basin, an interval much shorter than the duration of thrusting activity (Vergés *et al.* 1995).

The activity of the southern margin of the foreland basin, starting at 41.5 Ma, influenced

Table 3. *Comparison of subsidence results among different European foreland basins together with an estimation of the duration of the deep-marine stage and the shallow-marine and continental stage during the foreland basin infill. Maximum rates of tectonic subsidence are shown for localities in both proximal and distal positions with respect to the thrust front*

Locality	(EPD) Eastern Pyrenean basin	(JB) Jaca basin	(AB) Aquitaine basin	(SAB) Swiss Alpine basin	(GAB) German Alpine basin
Backstripping	Local		Local	Local	Flexural (EET = 48Km)
Reference	This work	Labaume *et al.* (1985) Barnolas & Teixell (1994)	Brunet *et al.* (1984) Dubarry (1988) Desegaulx *et al.* (1991)	Homewood *et al.* (1986) Pifner (1992)	Jin (1995)
Total duration	56–25 MaBP (31 Ma)	56–25 MaBP (31 Ma)	60–25 MaBP (35 Ma)	46–15 MaBP (31 Ma)	43–8 MaBP (35 Ma)
Marine stage	56–37 MaBP (19 Ma)	56–37 MaBP (19 Ma)	60–49 MaBP (11 Ma)	46–34 MaBP (12 Ma)	43–28 MaBP (15 Ma)
Continental stage	37–25 MaBP (12 Ma)	37–<25 MaBP (12 Ma)	49–>25 MaBP (24 Ma)	34–15 MaBP (19 Ma)	28–8 MaBP (20 Ma)
Maximum rates of tectonic subsidence (in mm a^{-1}): frontal-distal locality, at (x km of the front)					
Maximum rates	0.53–0.15 (at 60 km)		0.2–0.13 (at ≤15 km)	0.1–0.06	0.9–0.3 (at 60 km)
Flexure migration	c. 10 mm a^{-1}	5 mm a^{-1}	0.3–0.7 mm a^{-1}	9–2 mm a^{-1}	

the subsidence geometry of the basin, especially during the fourth depositional cycle as confirmed by the double flexure of the basin, represented in the geological cross-section. The end of important carbonate production during this last marine depositional cycle, coeval with the progradation of significant siliciclastic systems in the margins of the basin, marks the initial overfilled conditions of the whole basin although tectonic subsidence is still important.

Western European foreland basins developed during Tertiary times by the collision of continental plates flexed downward at a similar maximum tectonic rates of 0.6–0.9 mm a^{-1} close to the tectonic front and *c.* 0.1 mm/a^{-1} far away from it. Maximum rates of tectonic subsidence are about an order of magnitude smaller than rates of thrust front advance.

This local isostatic backstripping analysis represents a first step in the quantification of vertical motions in the south Pyrenean foreland basin, and it has to be improved at different scales. At a large scale, flexural rigidity of the Iberian crust during thrusting (Millán *et al.* 1995) has to be taken in account. For areas with irregular shapes like the Ebro basin where other margins affected the basin evolution, a 3D flexural backstripping analysis is necessary to determine the contributions of such margins to the tectonic subsidence within the basin. At basin scale the refinement of the chronostratigraphic framework of the Ebro foreland basin infill as well as the analysis of palaeobathymetric indicators is needed. Also a good correlation with refined sea-level curves would be necessary, especially at smaller scales of third order depositional cycles. The geometry of the deforming thrust front and its relation with syn-thrusting deposits are important to understand foreland basin depositional geometries during thrusting. It is important to discriminate tectonic thickening of the sedimentary succession due to layer parallel shortening, folding and thrusting in subsidence analysis. Indeed, determination of the relative position of successive analysed intervals with respect to the advancing thrust wedge deformation front is important to properly relate changes in subsidence trend with tectonic events. This only can be accomplished by the integration of detailed structural, stratigraphic and chronologic studies. Combination of subsidence and geochemical results is necessary to corroborate geohistories of sedimentary basins and especially to determine syn-thrusting and post-thrusting exhumation events.

We thank S. Crews who wrote the backstripping analysis program we used for our calculations, C. L. Angevine for useful comments about the program, and A. Permanyer for vitrinite reflectance analysis. We also thank to H.-P. Luterbacher and M. Séguret for constructive and critical reviews. This work was founded by IBS Project, Joule II Programme (JOU2-CT92-110), the 'Comissionat per Universitats i Recerca de la Generalitat de Catalunya', Quality Group GRQ94-1048, Total Exploration Production France and by grants from the National Science Foundation (EAR8816181, 9018951) and the Petroleum Research Fund (ACS-PRF 20591, 17625, 23881) to D.W.B.

References

ANGEVINE, C. L., P. L. HELLER, & PAOLA, C. 1990. *Quantitative Sedimentary Basin Modeling*. Continuing Education Course Note Series 32, American Association of Petroleum Geologists, Tulsa.

ALLEN, P. A. & ALLEN, J. R. 1990. *Basin Analysis*. Principles and Applications. Blackwell Scientific Publications, Oxford.

——, CRAMPTON, S. L. & SINCLAIR, H. D. 1991. The inception and early evolution of the North Alpine Foreland Basin, Switzerland. *Basin Research*, **3**, 143-163.

——, HOMEWOOD, P. & WILLIAMS, G. D. 1986. Foreland basins: an introduction. *In*: ALLEN, P. A. & HOMEWOOD, P. (eds) *Foreland Basins*. Special Publications of the International Association of Sedimentologists, **8**, 3–12.

BARNOLAS, A. 1992. Evolución sedimentaria de la Cuenca Surpirenaica Oriental durante el Eoceno. *Acta Geologica Hispànica*, **27**, 15–31.

BARNOLAS, A. & TEIXELL, A. 1994. Platform sedimentation and collapse in a carbonate-dominated margin of a foreland basin (Jaca basin, Eocene, southern Pyrenees). *Geology*, **22**, 1107–1110.

BARTRINA, M. T., CABRERA, L., JURADO, M. J., GUIMERÀ, J. & ROCA, E. 1992. Evolution of the central Catalan margin of the Valencia trough (western Mediterranean). *Tectonophysics,* **203**, 219–47.

BEAUMONT, C. 1981. Foreland basins. *Geophysical Journal of the Royal Astronomical Society*, **65**, 291–329.

BENTHAM, P. & BURBANK, D. W. 1996. Chronology of Eocene foreland basin evolution along the western oblique margin of the South-Central Pyrenees. *In*: FRIEND, P. F. & DABRIO, C. J. (eds) *Tertiary Basins of Spain*. Cambridge University Press, World and Regional Geology, **E11**, 144–152.

BURBANK, D. W., PUIGDEFÀBREGAS, C. & MUÑOZ, J. A. 1992*a*. The chronology of the Eocene tectonic and stratigraphic development of the eastern Pyrenean Foreland Basin, NE Spain. *Geological Society of America Bulletin*, **104**, 1101–1120.

——, VERGÉS, J., MUÑOZ, J. A. & BENTHAM, P. 1992*b*. Coeval hindward- and forward-imbricating thrusting in the Central Southern Pyrenees, Spain: Timing and rates of shortening and deposition. *Geological Society of America Bulletin*, **104**, 3–17.

CANDE, S. C. & KENT, D. V. 1995. Revised calibration

of the geomagnetic polarity timescale for the Late Cretaceous and Cenozoic. *Journal of Geophysical Research*, **100**, 6093–6095.

CASAS, J. M., DURNEY, D., FERRET, J. & MUÑOZ, J. A. 1996. Determinación de la deformación finita en la vertiente sur del Pirineo oriental a lo largo de la transversal del río Ter. *Geogaceta*, **20**, 803–805.

CHOUKROUNE, P. & ECORS TEAM 1989. The ECORS Pyrenean deep seismic profile reflection data and the overall structure of an orogenic belt. *Tectonics*, **8**, 23–39.

CLAVELL, E. 1992. *Geologia del petroli de les conques terciàries de Catalunya*. PhD Thesis, University of Barcelona.

CONEY, P. J., MUÑOZ, J. A., MCCLAY, K. R. & EVENCHICK, C. A. 1996. Syntectonic burial and post-tectonic exhumation of the southern Pyrenees foreland fold-thrust belt. *Journal of Geological Society, London*, **153**, 9–16.

DAIGNIÈRES, M., SÉGURET, M., SPETCH, M. & ECORS TEAM 1994. The Arzacq-Western Pyrenees ECORS Deep Seismic Profile. *In*: MASCLE, A. (ed.) *Hydrocarbon and Petroleum Geology of France*. Special Publication of the European Association of Petroleum Geoscientists, **4**, Springer-Verlag, 199–208.

DECELLES, P. G. & GILES, K. A. 1996. Foreland basin systems. *Basin Research*, **8**, 105–123.

DESEGAULX, P. & BRUNET, M.-F. 1990. Tectonic subsidence of the Aquitaine basin since Cretaceous times. *Bulletin de la Societe Geologique de France*, **8**, VI, n. 2, 295–306.

——, KOOI, H. & CLOETINGH, S. 1991. Consequences of foreland basin development on thinned continental lithosphere: application to the Aquitaine basin (SW France). *Earth and Planetary Science Letters*, **106**, 116–132.

DOROBEK, S. L. 1995. Synorogenic carbonate platforms and reefs in foreland basins: Controls on stratigraphic evolution and platform/reef morphology. *In*: DOROBEK, S. L. & ROSS, G. M. (eds) *Stratigraphic Evolution of Foreland Basins*. SEPM Special Publications, **52**, 127–147.

DUBARRY, R. 1988. *Interprétation dynamique du Paléocène et de l'Éocène inférieur et moyen de la région de Pau-Tarbes (avant-pays Nord des Pyrénées occidentales; SW France): sedimentologie, correlations diagraphiques, decomposition et calcul de subsidence*. PhD Thesis, University of Pau.

ECORS-CROP DEEP SEISMIC SOUNDING GROUP 1989. A new picture of the Moho under the western Alps. *Nature*, **337**, 249–251.

FERRER, J. 1971. *Le Paléocène et l'Eocène des Cordillerès Cotières de la Catalogne (Espagne)*. Mémoires Suisses de Paléontologie, **90**.

FLEMINGS, P. B. & JORDAN, T. E. 1989. Stratigraphic modeling of foreland basins: Interpreting thrust deformation and lithosphere rheology. *Geology*, **18**, 430–434.

GIMÉNEZ-MONTSANT, J. 1993. *Analisis de cuenca del Eoceno inferior de la Unidad Cadí (Pirineo oriental): El sistema deltaico y de plataforma carbonatica de la Formación de Corones*. PhD Thesis, University of Barcelona.

HAQ, B. U., HARDENBOL, J. & VAIL, P. R. 1987. Chronology of Fluctuating Sea Levels Since the Triassic. *Science*, **235**, 1156–1166.

HELLER, P. L., ANGEVINE, C. L. & WINSLOW, N. S. 1988. Two-phase stratigraphic model of foreland-basin sequences. *Geology*, **16**, 501–504.

HINE, A., LOCKER, S. D., TEDESCO, L. P., MULLINS, H. T., HALLOCK, P., BELKNAP, D. F., GONZALEZ, J. L., NEUMANN, A. C. & SNYDER, S.W. 1992. Megabreccias shedding from modern, low-relief carbonate platforms, Nicaraguan Rise. *Geological Society of America Bulletin*, **104**, 8, 928–943.

HOMEWOOD, P., ALLEN, P. A. & WILLIAMS, G. D. 1986. Dynamics of the Molasse Basin of western Switzerland. *In*: ALLEN, P. A. & HOMEWOOD, P. (eds) *Foreland Basins. Special Publications of the International Association of Sedimentologists*, **8**, 199–217.

HOTTINGER, L. 1960. *Recherches sur les Alvéolines du Paléocéne et de l'Eocéne*. Memoires Suisses de Paléontologie, **75–76**.

—— 1977. Distribution of larger foraminifera Peneroplidae, *Borelis*, and Nummulitidae in the Gulf of Elat, Red Sea. *In*: DROOGER, C. W. (ed.) *Depth-Relations of Recent Larger Foraminifera in the Gulf of Aqaba-Elat. Utrecht Micropaleontological Bulletin*, **15**, 35–109.

JIN, J. 1995. Dynamic stratigraphic analysis and modeling in the South-Eastern German Molasse Basin. *Tübingen Geowissenschaftliche Arbeiten*, **24**, 1–153.

JOHNS, D. R., MUTTI, E., ROSELL, J. & SÉGURET, M. 1981. Origin of a thick, redeposited carbonate bed in the Eocene turbidites of the Hecho Group, South-Central Pyrenees, Spain. *Geology*, **9**, 161–164.

JORDAN, T. E. 1981. Thrust loads and foreland basin evolution, Cretaceous, Western United States. *AAPG Bulletin*, **65**, 2506–2520.

—— & FLEMINGS, P. B. 1991. Large-scale stratigraphic arquitecture, eustatic variation, and unsteady tectonism: A theorical evaluation. *Journal of Geophysical Research*, **96**, 6681–6699.

LABAUME, P., SÉGURET, M. & SEYVE, C. 1985. Evolution of a turbiditic foreland basin and analogy with an accretionary prism: Example of the Eocene South-Pyrenean basin. *Tectonics*, **4**, 661–685.

LANAJA, J.M. 1987. *Contribución de la exploración petrolífera al conocimiento de la geología de España*. Instituto Geológico de España.

LEWIS, C. J., VERGÉS, J., MARZO, M. & HELLER, P. L. 1996. Youtfhful topography indicating active surface uplift in NE Iberia: Mantle upwelling along a leakly transform fault? *Annales Geophysicae*, Supplement I, **14**, C-204.

LÓPEZ-BLANCO, M. 1993. Stratigraphy and sedimentary development of the Sant Llorenç del Munt fan-delta complex (Eocene, southern Pyrenean foreland basin, northeast Spain). *In:* FROSTICK, L. E. & STEEL, R. J. (eds) *Tectonic Controls and Signatures in Sedimentary Successions*. Special Publications of the Association of Sedimentologists, **20**, 67–88.

LÓPEZ-BLANCO, M., MARZO, M., BURBANK, D.,

VERGÉS, J., ROCA, E., ANADÓN, P. & PIÑA, J. In press. Tectonic and climatic controls on the development of large, foreland fan deltas: Montserrat and Sant Llorenç del Munt systems (Middle Eocene, Ebro basin, NE Spain). *In*: MARZO, M. & STEEL, R. (eds) *Sedimentology and sequence stratigraphy of the Sant Llorenç del Munt clastic wedges (SE Ebro basin, NE Spain)*. Sedimentary Geology Special Issue,

LUTERBACHER, H. P., EICHENSEER, H., BETZLER, CH., & VAN DEN HURK, A. M. 1991. Carbonate-siliciclastic depositional systems in the Paleogene of the South Pyrenean foreland basin: a sequence-stratigraphic approach. *In*: MACDONALD, D. I. M. (ed.) *Sedimentation, Tectonics and Eustasy*. Special Publications of the International Association of Sedimentologists, **12**, 391–408.

MARTÍNEZ, A., VERGÉS, J., CLAVELL, E. & KENNEDY, J. 1989. Stratigraphic framework of the thrust geometry and structural inversion in the south-eastern Pyrenees: La Garrotxa area. *Geodinamica Acta*, **3**, 185–194.

——, —— & MUÑOZ, J. A. 1988. Secuencias de propagación del sistema de cabalgamientos de la terminación oriental del manto del Pedraforca y relación con los conglomerados sinorogénicos. *Acta Geologica Hispànica*, **23**, 119–128.

MATÓ, E., SAULA, E., VERGÉS, J., MARTÍNEZ-RÍUS, A., ESCUER, J. & BARBERÀ, M. 1994. *Mapa Geológico de España. Plan Magna a escala 1:50.000. Hoja de Berga (293)*. Instituto Tecnológico Geominero de España, Madrid.

MEIGS, A., VERGÉS, J. & BURBANK, D. W. 1996. Ten-million-year history of a thrust sheet. *Geological Society of America Bulletin*.

MILLÁN, H., DEN BEZEMER, T., VERGÉS, J., ZOETEMEIJER, R., CLOETINGH, S., MARZO, M, MUÑOZ, J. A., PUIGDEFÀBREGAS, C., ROCA, E. & CIRÉS, J. 1995. Present-day and Middle Lutetian flexural modelling in the Eastern Pyrenees and Ebro Basin. *Marine and Petroleum Geology*, **12**, 917–928.

MUÑOZ, J.A. 1992. Evolution of a Continental Collision Belt: ECORS-Pyrenees Crustal Balanced Cross-section. *In*: MCCLAY, K. (ed.) *Thrust Tectonics*. Chapman & Hall, London, 235–246.

——, MARTÍNEZ, A. & VERGÉS, J. 1986. Thrust sequences in the eastern Spanish Pyrenees. *Journal of Structural Geology*, **8**, 399–405.

——, VERGÉS, J., MARTÍNEZ-RÍUS, A., FLETA, J., CIRÉS, J., CASAS, J. M. & SÀBAT, F. 1994. *Mapa Geológico de España. Plan Magna a escala 1:50.000. Hoja de Ripoll (256)*. Instituto Tecnológico Geominero de España, Madrid.

ORTÍ, F., BUSQUETS, P., ROSELL, L., TABERNER, C., UTRILLA, R. & QUADRAS, M. 1988. La fase evaporítica del Eoceno medio (Luteciense) en la cuenca surpirenaica catalana. Nuevas aportaciones. *Revista d'Investigacions Geològiques*, **44-45**, 281–302.

PEPER, T. 1993. *Tectonic control on the sedimentary record in foreland basins: inferences from quantitative subsidence analyses and stratigraphic modelling*. PhD. Thesis Vrije Univesitet, Amsterdam.

PERMANYER, A., VALLÉS, D. & DORRONSORO, C. 1988. Source Rock potential of an Eocene carbonate slope: the Armàncies Formation of the Southern Pyrenean Basin, Northeast Spain, *AAPG Bulletin*, **72**, 1019.

PFIFFNER, A. 1992. Alpine orogeny. *In*: BLUNDELL, D., FREEMAN, R. & MUELLER, S. (eds) *A continent revealed. The European Geotraverse*. Cambridge University press, 180–190.

PRICE, R. A. 1973. Large-scale gravitational flow of supr-crustal rocks, southern Canadian Rockies *In*: DE JONG, K. A. & SCHOLTEN, R. A. (eds) *Gravity and Tectonics*. Wiley, New York, 491–502.

PUIGDEFÀBREGAS, C., MUÑOZ, J. A. & MARZO, M. 1986. Thrust belt development in the Eastern Pyrenees and related depositional sequences in the southern foreland basin. *In*: ALLEN, P. A. & HOMEWOOD, P. (eds.) *Foreland Basins*. Special Publications of the International Association of Sedimentologists, **8**, 229–246.

——, —— & VERGÉS, J. 1992. Thrusting and Foreland Basin Evolution in the Southern Pyrenees. *In*: MCCLAY, K. (ed.) *Thrust Tectonics*. Chapman & Hall, London, 247–254.

PUJALTE, V., BACETA, J. I., PAYROS, A., ORUE-ETXEBARRIA, S & SERRA-KIEL, J. 1994. *Late Cretaceous–Middle Eocene Sequence Stratigraphy and Biostratigraphy of the SW and W Pyrenees (Pamplona and Basque Basins, Spain)*. G.E.P. and IGCP Project 286, Field Seminar.

ROCA, E. 1992. *L'estructura de la conca Catalano-Balear: paper de la compressió i de la distensió en la seva gènesi*. PhD. Thesis, University of Barcelona.

REISS, Z. & HOTTINGER, L. 1984. *The Gulf of Aqaba. Ecological micropaleontology*. Ecological studies **50**. Springer Verlag.

RICCI LUCCHI, F. 1986. The Oligocene to Recent foreland basins of the northern Apennines. *In*: ALLEN, P. A. & HOMEWOOD, P. (eds) *Foreland Basins*. Special Publications of the International Association of Sedimentologists, **8**, 105–139.

RIVERO, L. 1993. *Estudio Gravimétrico del Pirineo Oriental*. PhD Thesis, University of Barcelona.

SAMSÓ, J. M., SERRA-KIEL, J., TOSQUELLA, J. & TRAVÉ, A. 1994. Cronostratigrafía de las plataformas lutecienses de la zona central de la cuenca surpirenaica. *In*: MUÑOZ, A., GONZALEZ, A. & PÉREZ, A. (eds) *II Congreso Grupo Español del Terciario, Comunicaciones, Jaca*, 205–208.

SANS, M., MUÑOZ, J.A. & VERGÉS, J. 1996. Thrust wedge geometries related to evaporitic horizons (Southern Pyrenees). *Bulletin of Canadian Petroleum Geology*, **44**, 375–384.

SAULA, E., MATÓ, E., ESCUER, J., MUÑOZ, J. A. & BARNOLAS, A. 1994. *Mapa Geologico de España. Plan Magna a escala 1:50.000, Hoja de Manlleu (294)*. Instituto Tecnológico Geominero de España, Madrid.

SCHAUB, H. 1981. *Nummulites et Assilines de la Téthys Paleogène. Taxinomie, phylogenese et biostratigraphie*. Memoires Suisses Paléontologie, **104–106**.

SCLATER, J. G. & CHRISTIE, P. A. F. 1980. Continental

stretching: an explanation of the post Mid-Cretaceous subsidence of the Central North Sea basin. *Journal of Geophysical Research*, **85**, 3711–3739.

SÉGURET, M. 1972. *Étude tectonique des nappes et séries décollées de la partie centrale du versant sud des Pyrénées*. Publication USTELA, série Geologie structurale, **2**. Montpellier.

SERRA-KIEL, J. 1984. *Estudi dels Nummulites del grup N. perforatus (Monfort)*. Treballs de la Institut Catalan d'Historia Natural, **11**.

—— & TRAVÉ, A. 1995. Lithostratigraphic and chronostratigraphic framework of the Bartonian sediments in the Vic and Igualada areas. *In*: PEREJÓN, J. A. & BUSQUESTS, P. (eds) *VII International Symposium Fossil Cnidaria and Porifera*, Madrid, 11–14.

——, CANUDO, J. I., DINARÈS, J., MOLINA, E., ORTÍZ, N., PASCUAL, J. O., SAMSÓ, J. M. & TOSQUELLA, J. 1994. Cronoestratigrafía de los sedimentos marinos del Terciario inferior de la Cuenca de Graus-Tremp (zona Central Surpirenaica). *Revista de la Soceologel Geologica España*, **7**, 273–297.

——., HOTTINGER, L., DROBNE, K., FERRÁNDEZ, C., LESS, G., JAUHRI, A. K., PIGNATTI, J., SAMSÓ, J. M., SCHAUB, H., SIREL, E., TAMBAREAU, Y., TOSQUELLA, J. & ZAKREVSKAYA, E. *in press*. Benthic Foraminifera from Paleocene and Eocene. *In*: DE GRACIANSKY, P. C., HARDENBOL, J., JACQUIN, T. & VAIL, P. R. (eds) *Mezosoic-Cenozoic Sequence Stratigraphy of Western European Basins*. SEPM Special Publications, **00**, 00–00.

SINCLAIR, H. D. & ALLEN, P. 1992. Vertical versus horizontal motions in the Alpine orogenic wedge: stratigraphic response in the foreland basin. *Basin Research*, **4**, 215–232.

——, COAKLEY, B. J., ALLEN, P. A. & WATTS, A. B. 1991. Simulation of foreland basin stratigraphy using a difusion model of mountain belt uplift and erosion: an example from Central Alps, Switzerland. *Tectonics*, **10**, 599–620.

SONNENFELD, P. 1984. *Brines and evaporites*. Academic Press Inc., Orlando, Florida.

STECKLER, M. S. & WATTS, A. B. 1978. Subsidence of the Atlantic type continental margin of New York, *Earth and Planetary Science Letters*, **42**, 1–13.

TEIXELL, A. 1996. The Ansó transect of the southern Pyrenees: basement and cover thrust geometries. *Journal of the Geological Society, London*, **153**, 301–310.

TOSQUELLA, J. 1995. *Els Nummulitinae del Paleocè-Eocè inferior de la conca sudpirinenca*. PhD Thesis, University of Barcelona.

VAIL, P. R., MITCHUM, R. M. & THOMPSON, S. 1977. Seismic stratigraphy and global changes of sea level, part 3: relative change of sea level from coastal onlap. *In*: PAYTON, C. A. (ed.) *Seismic Stratigraphy - applications to hydrocarbon exploration*, AAPG Memoirs, **26**, 63–81.

VAN HINTE, J. E. 1978. Geohistory analysis-application of micropalaeontology in exploration geology. *AAPG. Bulletin*, **62**, 201–222.

VERGÉS, J. 1993. *Estudi geològic del vessant sud del Pirineu oriental i central. Evolució cinemàtica en 3D*. PhD Thesis, University of Barcelona.

—— & BURBANK, D. W. 1996. Eocene-Oligocene thrusting and basin configuration in the eastern and central Pyrenees (Spain). *In*: FRIEND, P .F. & DABRIO, C. J. (eds) *Tertiary Basins of Spain*. Cambridge University Press, World and Regional Geology, **E11**, 120–133.

—— & MARTÍNEZ, A. 1988. Corte compensado del Pirineo oriental: geometria de las cuencas de antepaís y edades de emplazamiento de los mantos de corrimiento. *Acta Geologica Hispànica*, **23**, 95–106.

——, MARTÍNEZ-RÍUS, A., DOMINGO, F., MUÑOZ, J. A., LOSANTOS, M., FLETA, J. & GISBERT, J. 1994. *Mapa Geológico de España. Plan Magna a escala 1:50.000. Hoja de La Pobla de Lillet (255)*. Instituto Tecnológico Geominero de España, Madrid.

——, MILLÁN, H., ROCA, E., MUÑOZ, J. A., MARZO, M., CIRÉS, J., DEN BEZEMER, T., ZOETEMEIJER, R. & CLOETINGH, S. 1995. Eastern Pyrenees and related foreland basins: pre-, syn- and post-collisional crustal-scale cross-sections. *Marine and Petroleum Geology*, **12**, 903–916.

——, MUÑOZ, J. A. & MARTÍNEZ, A. 1992. South Pyrenean fold-and-thrust belt: Role of foreland evaporitic levels in thrust geometry. *In*: MCCLAY, K. (ed.) *Thrust Tectonics*. Chapman & Hall, London, 255–264.

ZOETEMEIJER, R., SASSI, W., ROURE, F. & CLOETINGH, S. 1992. Stratigraphic and kinematic modelling of thrusts evolution, northern Apennines, Italy. *Geology*, **20**, 1035–1038.